PML-NB-dependent type I interferon memory results in a restricted form of HSV latency

Jon B. Suzich[1], Sean R. Cuddy[2], Hiam Baidas[1], Sara Dochnal[1], Eugene Ke[1], Austin R. Schinlever[1], Aleksandra Babnis[1], Chris Boutell[3] and Anna R. Cliffe[1]*

1. Department of Microbiology, Immunology and Cancer Biology, University of Virginia, Charlottesville, VA, 22908.
2. Neuroscience Graduate Program, University of Virginia, Charlottesville, VA, 22908
3. MRC-University of Glasgow Centre for Virus Research (CVR), Garscube Campus, Glasgow, Scotland, United Kingdom

* Correspondence to Anna R. Cliffe, cliffe@virginia.edu

Keywords: HSV, Interferon, PML-NB, Latency, Neuron

Abstract

Herpes simplex virus (HSV) establishes latent infection in long-lived neurons. During initial infection, neurons are exposed to multiple inflammatory cytokines but the effects of immune signaling on the nature of HSV latency is unknown. We show that initial infection of primary murine neurons in the presence of type I interferon (IFN) results in a form of latency that is restricted for reactivation. We also find that the subnuclear condensates, promyelocytic leukemia-nuclear bodies (PML-NBs), are absent from primary sympathetic and sensory neurons but form with type I IFN treatment and persist even when IFN signaling resolves. HSV-1 genomes colocalize with PML-NBs throughout a latent infection of neurons only when type I IFN is present during initial infection. Depletion of PML prior to or following infection does not impact the establishment latency; however, it does rescue the ability of HSV to reactivate from IFN-treated neurons. This study demonstrates that viral genomes possess a memory of the IFN response during *de novo* infection, which results in differential subnuclear positioning and ultimately restricts the ability of genomes to reactivate.

Introduction

Herpes simplex virus-1 (HSV-1) is a ubiquitous pathogen that persists in the form of a lifelong latent infection in the human host. HSV-1 can undergo a productive lytic infection in a variety of cell types; however, latency is restricted to post-mitotic neurons, most commonly in sensory, sympathetic and parasympathetic ganglia of the peripheral nervous system (Baringer & Pisani, 1994; Baringer & Swoveland, 1973; Richter *et al*, 2009; Warren *et al*, 1978). During latent infection, the viral genome exists as an episome in the neuronal nucleus, and there is considerable evidence that on the population level viral lytic gene promoters assemble into repressive heterochromatin (Cliffe *et al*, 2009; Cliffe & Knipe, 2008; Kwiatkowski *et al*, 2009; Wang *et al*, 2005). The only region of the HSV genome that undergoes active transcription, at least in a fraction of latently infected cells, is the latency associated transcript (LAT) locus (Kramer & Coen, 1995; Stevens *et al*, 1987). Successful establishment of a latent gene expression program requires a number of molecular events, likely influenced by both cellular and viral factors, and is not uniform (Efstathiou & Preston, 2005). Significant heterogeneity exists in expression patterns of both lytic and latent transcripts in latently-infected neurons, as well as in the ability of latent genomes to reactivate in response to different stimuli (Catez *et al*, 2012; Ma *et al*, 2014; Maroui *et al*, 2016; Nicoll *et al*, 2016; Proenca *et al*, 2008; Sawtell, 1997). This heterogeneity could arise from viral genome copy number, exposure to different inflammatory environments or intrinsic differences in the neurons themselves. Furthermore, there is growing evidence that heterogeneity in latency may ultimately be reflected in part by the association of viral genomes with different nuclear domains or cellular proteins (Catez *et al.*, 2012; Maroui *et al.*, 2016).

However, what determines the subnuclear distribution of latent viral genomes is not known. In addition, it is currently unclear whether viral genome association with certain nuclear domains or cellular proteins results in an increased or decreased ability of the virus to undergo reactivation. The aim of this study was to determine whether the presence of interferon during initial HSV-1 infection can intersect with the latent viral genome to regulate the type of gene silencing and ultimately the ability to undergo reactivation. Because the fate of viral genomes and their ability to undergo reactivation can be readily tracked, latent HSV-1 infection of neurons also serves as an excellent system to explore how exposure to innate immune cytokines can have a lasting impact on peripheral neurons.

Latent HSV-1 genomes have been shown to associate with Promyelocytic leukemia nuclear bodies (PML-NBs) in mouse models of infection, as well as in human autopsy material (Catez *et al.*, 2012; Maroui *et al.*, 2016). PML-NBs are heterogenous, phase-separated nuclear condensates that have been associated with the transcriptional activation of cellular genes (Bernardi & Pandolfi, 2007; Kim & Ahn, 2015; Lallemand-Breitenbach & de The, 2010; McFarlane *et al*, 2019; Wang *et al*, 2004), but also can recruit repressor proteins, including ATRX, Daxx and Sp100, that promote transcriptional repression and inhibition of both DNA and RNA virus replication (Bishop *et al*, 2006; Everett & Chelbi-Alix, 2007; Garrick *et al*, 2004; Xu & Roizman, 2017; Zhong *et al*, 2000b). In the context of lytic infection of non-neuronal cells, PML-NBs have been shown to closely associate with HSV-1 genomes (Maul, 1998; Maul *et al*, 1996), and the HSV-1 viral regulatory protein ICP0 is known to disrupt the integrity of

these structures by targeting PML and other PML-NB associated proteins for degradation (Boutell *et al*, 2002; Chelbi-Alix & de The, 1999; Everett & Maul, 1994). PML-NBs entrapment of HSV-1 genomes during lytic infection of fibroblasts (Alandijany *et al*, 2018) is hypothesized to create a transcriptionally repressive environment for viral gene expression, as PML directly contributes to the cellular repression of ICP0-null mutant viruses (Everett *et al*, 2006). In the context of latency, neurons containing PML-encased latent genomes exhibit decreased expression levels of the LAT (Catez *et al.*, 2012), suggesting that they are more transcriptionally silent than latent genomes localized to other nuclear domains and raising the question as to whether PML-NB-associated genomes are capable of undergoing reactivation. Studies have shown that replication-defective HSV genomes associated with PML-NBs are capable of derepressing following induced expression of ICP0 in fibroblasts (Cohen *et al*, 2018; Everett *et al*, 2007) and following addition of the histone deacetylase inhibitor trichostatin A (TSA) in cultured adult TG neurons (Maroui *et al.*, 2016). However, it is not known if replication-competent viral genomes associated with PML-NBs are capable of undergoing reactivation triggered by activation of cellular signaling pathways in the absence of viral protein.

PML-NBs can undergo significant changes in number, size and localization depending on cell type, differentiation stage and cell-cycle phase, as well as in response to cellular stress and soluble factors (Bernardi & Pandolfi, 2007; Lallemand-Breitenbach & de The, 2010). Interferon (IFN) treatment directly induces the transcription of PML, Daxx, Sp100 and other PML-NB constituents, which leads to

elevated protein synthesis and a robust increase in both size and number of PML-NBs (Chelbi-Alix *et al*, 1995; Greger *et al*, 2005; Grotzinger *et al*, 1996; Shalginskikh *et al*, 2013; Stadler *et al*, 1995). During HSV-1 infection, type I IFNs are among the first immune effectors produced, and they have been shown to restrict HSV viral replication and spread both *in vitro* and *in vivo* through multiple pathways (Hendricks *et al*, 1991; Jones *et al*, 2003; Mikloska & Cunningham, 2001; Mikloska *et al*, 1998; Sainz & Halford, 2002). Type I IFNs are elevated within peripheral ganglia during HSV-1 infection (Carr *et al*, 1998) and have been linked with control of lytic HSV-1 replication. In an *in vitro* model of latency, exogenous type I IFNs also have been shown to induce neuron-specific anti-viral responses that control reactivation (Linderman *et al*, 2017), but whether type I IFN exposure during initial infection modulates entry into latency is not known. Importantly, exposure to IFN and other cytokines has also been shown to generate innate immune memory or 'trained immunity' in fibroblasts and immune cells (Kamada *et al*, 2018; Moorlag *et al*, 2018), and PML-NBs themselves are potentially important in the host innate immune response. A previous study found that the histone chaperone HIRA is re-localized to PML-NBs in response to the innate immune defenses induced by HSV-1 infection, and in this context, PML was required for the recruitment of HIRA to ISG promoters for efficient transcription (McFarlane *et al.*, 2019). Prior exposure to type I interferons has also been shown to promote a transcriptional memory response in fibroblasts and macrophages (Kamada *et al.*, 2018). This interferon memory lead to faster and more robust transcription of ISGs following restimulation and coincided with acquisition of certain chromatin marks and accelerated recruitment of transcription and chromatin factors (Kamada *et al.*, 2018). Thus far, long term memory

of cytokine exposure has only been investigated in non-neuronal cells, but it is conceivable that neurons, being non-mitotic and long-lived cells, also possess unique long-term responses to prior cytokine exposure.

Although *in vivo* models are incredibly powerful tools to investigate the contribution of the host immune response to HSV infection, they are problematic for investigating how individual components of the host's immune response specifically regulate neuronal latency. Conversely, *in vitro* systems provide a simplified model that lack many aspects of the host immune response. Therefore, to investigate the role of type I IFN on HSV-1 latency and reactivation, we utilized a model of latency in primary murine sympathetic neurons (Cliffe *et al*, 2015), which allowed us to manipulate conditions during initial HSV-1 infection and trigger synchronous robust reactivation. Using this model, we show that primary neurons isolated from mouse peripheral ganglia are largely devoid of detectable PML-NBs but PML-NBs form following type I IFN exposure and persist even when ISG gene expression and production of other antiviral proteins have returned to baseline. Neither exogenous type I IFN nor detectable PML-NBs are required for HSV gene silencing and entry into latency in this model system, but, importantly, the presence of IFNα specifically at the time of initial infection results in the entrapment of viral genomes in PML-NBs and a more restrictive form of latency that is less able to undergo reactivation. This study therefore demonstrates how the viral latent genome has a long-term memory of the innate response during *de novo* HSV infection that results in entrapment of genomes in PML-NBs and a more repressive form of latency.

Results

Interferon induces the formation of detectable PML-NBs in primary sympathetic and sensory neurons isolated from postnatal and adult mice.

We initially set out to investigate the contribution of PML-NBs to HSV latency and reactivation using primary sympathetic and sensory neurons that have been well characterized as *in vitro* models of HSV latency and reactivation (Camarena *et al*, 2010; Cliffe *et al.*, 2015; Cuddy *et al*, 2020; Ives & Bertke, 2017; Wilcox & Johnson, 1987; Wilcox *et al*, 1990). In addition, primary neuronal systems allow for much more experimental control of specific conditions during *de novo* infection and can be easily manipulated either immediately prior to or following infection. Peripheral neurons were isolated from the superior cervical ganglia (SCG) or trigeminal ganglia (TG) from young (post-natal day; P1) or adult (>P28) mice and cultured for 6 days prior to staining. PML-NBs were defined as detectable punctate nuclear structures by staining for PML protein. Strikingly, we observed that both SCG and TG neurons were largely devoid of detectable PML-NBs (Fig. 1A).

In certain cell types, the transcription of certain PML-NB associated proteins, including PML, can be induced by either type I or type II interferon (IFN) treatment, which is correlated with an increase in PML-NB size and/or number per cell (Chelbi-Alix *et al.*, 1995; Stadler *et al.*, 1995). Therefore, we were interested in determining whether exposure of primary sensory or sympathetic neurons to different types of IFN resulted in PML-NB formation. Type I IFN treatment using IFN-alpha (IFNα) (Fig. 1B, 1C-1F) or IFN-beta (Fig. EV1A) led to a significant induction of detectable PML-NBs in both

sensory and sympathetic neurons isolated from postnatal and adult mice. Representative images of IFNα-treated neurons are shown (Fig. 1B) and number of detectable PML-NBs per neurons are quantified (Fig. 1C-1F). The increase in detectable PML-NBs was comparable for both 150 IU/ml and 600 IU/ml of IFNα. Type II IFN (IFNγ) led to a more variable response with a small but significant increase in detectable PML-NBs in a subpopulation of sympathetic neurons. However, IFNγ treatment of sensory neurons did not result in the formation of detectable PML-NBs. Exposure of neurons to IFN-lambda 2 (IFN-λ2), a type III IFN, did not induce the formation of detectable PML-NBs in either sympathetic or sensory neuron cultures (Fig. 1C-1F; Fig. EV1B,C). Therefore, PML-NBs are largely undetectable in primary sympathetic and sensory neurons but can form upon exposure to type I IFNs.

The absence of detectable PML-NBs in untreated primary neurons prompted us to investigate other known components of PML-NBs. We were particularly interested in ATRX and Daxx because like PML they have previously been found to be involved in restricting HSV lytic replication in non-neuronal cells (Alandijany *et al.*, 2018; Cabral *et al*, 2018; Lukashchuk & Everett, 2010; McFarlane *et al.*, 2019). Therefore, we investigated the localization of ATRX and Daxx in primary peripheral neurons. ATRX is a multifunctional, heterochromatin associated protein that is localized to PML-NBs in human and mouse mitotic cells and is largely characterized as interacting with the Daxx histone chaperone (Clynes *et al*, 2013; Lewis *et al*, 2010). In untreated neurons, we observed abundant ATRX staining throughout the nucleus in regions that also stained strongly with Hoechst (Fig. EV1D, E). This potential co-localization of ATRX with

206 regions of dense chromatin is consistent with a previous study demonstrating that in
207 neurons ATRX binds certain regions of the cellular genome associated with the
208 constitutive heterochromatin modification H3K9me3 (Noh *et al*, 2015). Importantly, this
209 distribution of ATRX differs from what is seen in murine dermal fibroblasts (Fig. EV1D,
210 E) and other non-neuronal cells, where there is a high degree of colocalization between
211 ATRX and PML (Alandijany *et al.*, 2018). Following treatment with IFNα, we found a
212 redistribution of ATRX staining and colocalization between ATRX and the formed PML-
213 NBs, but the majority of ATRX staining remained outside the context of PML-NBs (Fig.
214 EV1D, E). Similar to PML, sympathetic SCG and sensory TG neurons isolated from
215 both postnatal and adult mice were devoid of detectable puncta of Daxx staining (Fig.
216 EV1E), and we did not observe extensive Daxx staining in untreated neurons as we did
217 for ATRX. We were unable to directly co-stain for Daxx and PML; however, treatment of
218 neurons with IFNα did induce punctate Daxx staining that strongly colocalized with
219 puncta of ATRX (Fig. EV1E), which given our previous observation of ATRX co-
220 localization with PML following type I IFN treatment we used as a correlate for PML-
221 NBs. We were also interested in SUMO-1, which has been shown to be required for
222 formation of PML-NBs (Zhong *et al*, 2000a). Similar to ATRX and Daxx, treatment of
223 neurons with IFNα induced punctate SUMO-1 staining in P6 SCG neurons that
224 colocalized with PML puncta (Fig. EV1F). Therefore, PML-NBs containing their well
225 characterized associated proteins are not detected in cultured primary neurons but form
226 in response to type I IFN exposure.
227

228 Type I IFN treatment specifically at time of infection restricts reactivation of HSV-1 from
229 primary sympathetic neurons without affecting initial infectivity or LAT expression.
230 Because we observed that primary SCG neurons are largely devoid of PML-NBs
231 and that PML-NBs form upon treatment with type I IFN treatment, we first wanted to
232 clarify that latency was maintained in the absence of IFN and presumably without PML-
233 NB formation, consistent with our previous data (Cuddy *et al.*, 2020). SCG neurons
234 were infected at a multiplicity of infection (MOI) of 7.5 plaque forming units (PFU)/cell
235 with HSV-1 Us11-GFP presence of acyclovir (ACV). The ACV was removed after 6
236 days and the neuronal cultures were monitored to ensure the no GFP-positive neurons
237 were present (Fig. 2A). We found that latency could be established and maintained for
238 up to 5 days following removal of ACV (Fig. 2B). Reactivation was triggered by PI3K
239 inhibition using LY294002, as previously described (Camarena *et al.*, 2010; Cliffe *et al.*,
240 2015; Kim *et al*, 2012; Kobayashi *et al*, 2012), and quantified based on the number of
241 Us11-GFP neurons in the presence of WAY-150138 which blocks packaging of progeny
242 genomes and thus cell-to-cell spread (van Zeijl *et al*, 2000). These data therefore
243 indicate that exogenous IFN is not required to induce a latent state in this model
244 system.
245
246 We next turned our attention to whether type I IFN treatment at the time of
247 infection impacted the ability of HSV to establish latency or reactivate in this model
248 system. SCG neurons were pre-treated with IFNα (600 IU/ml) for 18h and during the
249 initial 2h HSV inoculation. Following inoculation, IFNα was washed out and an IFNAR1
250 blocking antibody was used to prevent subsequent type I IFN signaling through the

receptor. To confirm the effectiveness of the IFNAR1 ab to block detectable IFN signaling, we validated it by its ability to block ISG expression (ISG15) in cultured SCG neurons by RT-qPCR (Figure EV2A). Reactivation was induced and initially quantified based on the number of GFP positive neurons at 3-days post-stimuli. We found that full reactivation was restricted in neurons exposed to type I IFN just prior to and during *de novo* infection (Fig. 2C). We further confirmed this IFNα-mediated restriction of latency by the induction of lytic mRNAs upon reactivation. IFNα treatment at the time of infection significantly decreased the expression of immediate early gene (ICP27), early gene (ICP8) and late gene (gC) at 3 days post-reactivation (Fig. 2D, EV2B, C). There were very few GFP-positive neurons and little to no viral gene expression in mock reactivated controls, further indicating that latency can be established in the presence and absence of IFN.

Reactivation of HSV in this system proceeds over two phases. GFP-positive neurons is a readout for full reactivation or Phase II. However, we and others have observed an initial wave of lytic gene expression that occurs prior to and independently of viral DNA replication at around 20 hours post-stimulus, termed Phase I (Cliffe *et al.*, 2015; Cliffe & Wilson, 2017; Du *et al*, 2011; Kim *et al.*, 2012). Therefore, to determine if IFNα treatment at the time of infection restricted the Phase I wave of lytic we carried out RT-qPCR to detect representative immediate-early (ICP27), early (ICP8), and late (gC) transcripts at 20 hours post addition of LY294002. We found significantly decreased expression in the IFNα-treated neurons (Fig. 2E, EV2D, E). This is interesting as exogenous type I IFNs have previously been shown to suppress reactivation in murine neurons by preventing Phase I and are rendered ineffective once Phase I viral products accumulate (Linderman *et al.*, 2017). Therefore, type I IFN treatment solely at the time

of infection has a long-term effect on the ability of HSV to initiate lytic gene expression and undergo reactivation.

Because IFN treatment could reduce nuclear trafficking of viral capsids during initial infection or impact infection efficiency, we next determined whether equivalent numbers of viral genomes were present in the neuronal cultures. At 8dpi, we measured relative viral DNA genome copy numbers in SCG neurons that were treated with IFNα compared to untreated controls and found no significant difference (Fig 2F). To further confirm that equivalent genomes were present in the neuronal nuclei, we infected neurons with HSV-1 containing EdC-incorporated genomes and performed click chemistry to detect vDNA foci. At 8 dpi, we found no significant difference in the average number of vDNA foci per nucleus of neurons treated with IFNα at the time of initial infection compared to untreated controls (Fig. 2G). Therefore, the restricted reactivation phenotype mediated by IFNα was not due to a decrease in the number of latent viral genomes.

The decreased reactivation observed with IFNα treatment could be secondary to changes in expression of the LAT and/or directly as a result of decreased viral genome accessibility. The HSV LAT, one of the only highly expressed gene products during latent infection, has been shown to modulate several features of latency, including the viral chromatin structure, lytic gene expression, and neuronal survival, as well as the efficiency of latency establishment and reactivation (Chen *et al*, 1997; Garber *et al*, 1997; Gordon *et al*, 1995; Hill *et al*, 1990; Knipe & Cliffe, 2008; Leib *et al*, 1989; Perng

298 *et al*, 2000; Thompson & Sawtell, 1997, 2001; Trousdale *et al*, 1991). Therefore, the
299 ability of HSV to undergo reactivation could be due to changes in LAT expression
300 following IFNα treatment. However, when we evaluated LAT expression levels at 8 dpi
301 by RT-qPCR, we found no detectable difference between IFNα-treated and untreated
302 cultures of neurons. This suggests that the IFNα-mediated restriction in reactivation
303 does not appear to occur as a result of changes in expression of the LAT (Fig. 2H).
304 Therefore, it is possible that the type I IFN-mediated restriction of HSV latency is due to
305 changes to the latent genome that results in a decreased ability to undergo reactivation
306 following PI3-kinase inhibition.
307
308 Primary neurons have a memory of prior IFNα exposure characterized by persistence of
309 PML-NBs
310 Because we observed a restriction in the ability of HSV to reactivate that
311 occurred 7-8 days following type I IFN exposure, we went on to examine any long-term
312 changes resulting from IFNα exposure. First, we investigated the kinetics of
313 representative ISG expression. As expected, we saw a robust induction of *Isg15* and
314 *Irf7* in IFNα-treated (600 IU/ml) neurons that persisted for at least 42 hours post-
315 treatment post-addition of IFNα (this represents 1-day post-infection (dpi)). However, by
316 8 dpi, the time at which neurons were induced to reactivate, there was no detectable
317 difference in *Isg15* or *Irf7* expression in IFNα treated neurons vs untreated controls (Fig.
318 3A, B), indicating that these representative ISGs were not detectably elevated at the
319 time of reactivation. We also found similar *Isg15* and *Irf7* expression in HSV-1 infected
320 neurons compared to uninfected controls, suggesting that HSV-1 infection was not

impacting IFN signaling pathways at a population level. PML has been previously characterized as an ISG product in non-neuronal cells (Chelbi-Alix *et al.*, 1995; Stadler *et al.*, 1995) and is responsive to both IFNβ and IFNγ in latently-infected rat sympathetic neurons induced to reactivate (Linderman *et al.*, 2017), and we found an approximate 5-fold-increased expression of *Pml* in primary sympathetic neurons following IFNα treatment which was less than the increased expression of *Irf7* and *Isg15* (approximate 250-fold- and 100-fold-increased expression respectively). *Pml* expression returned to untreated levels by 1 dpi (Fig. 3C).

Although we did not detect maintained induction of IFN stimulated gene expression including *Pml*, we were intrigued as to whether PML-NBs persisted throughout the course of infection. To assess this, we first established whether PML-NBs persist even in the absence of sustained ISG expression. Quantifying the number of PML-NBs following IFNα (600 IU/ml) treatment, we found that the number of bodies remain elevated through 15 days post-treatment (Fig. 3D). We went on to investigate additional products of ISGs including STAT1 and Mx1 because of the availability of specific antibodies against these proteins. We observed robust STAT1 staining following IFNα exposure for 18 hours. However, by 8 days post infection we could not detect STAT1 staining in primary neurons indicating that accumulation of this IFNα-induced protein had returned to baseline (Fig. 3E). Similarly, we found induction of punctate Mx1 staining in neurons exposed to IFNα for 18 hours that was undetectable by day 6 post-treatment (Fig. 3F). Therefore, exposure of primary neurons to type I IFN led to a modest induction of *Pml* mRNA but resulted in long-term persistence of PML-

NBs, even in the absence of continued IFN signaling and when antiviral protein products of other ISGs were undetectable.

PML-NBs Persist and Stably Entrap Latent HSV-1 Genomes only if IFNα is Present at the Time of Initial Infection

The persistence of PML-NBs following IFN exposure raised the possibility that viral genomes are maintained within PML-NBs only in type I IFN-treated neurons. This would also suggest that PML-NB-associated genomes are less permissive for reactivation and provide us with an experimental system to investigate the contribution of PML-NBs to the maintenance of HSV latency. To determine whether viral genomes localize with PML-NBs in type I IFN-treated neurons, SCG neurons were pretreated with IFNα (600 IU/ml) then infected with HSV-1^{EdC} at an MOI of 5 PFU/cell in the presence of ACV and IFNα as described above. By co-staining for PML, we found that a large proportion of vDNA foci colocalized with PML-NBs in the IFNα-treated neurons over the course of infection. In untreated neurons that are largely devoid of detectable PML-NBs, very few genomes were colocalized to PML puncta as expected. Representative images are shown (Fig. 4A) and the percent of genome foci colocalized to PML-NBs is quantified (Fig. 4B). Furthermore, high-resolution Airy scan-based 3D confocal microscopy of IFNα-treated neurons revealed that vDNA foci were entrapped within PML-NBs (Fig. 4C, D), as has also been reported upon lytic infection of non-neuronal cell lines (Alandijany *et al.*, 2018) and in latently infected TG *in vivo* (Catez *et al.*, 2012), and interestingly, we found that the volume of PML-NBs associated with vDNA is greater than PML-NBs not associated with vDNA (Fig. 4E). Previous studies have found

that colocalization of viral DNA by PML-NBs during lytic HSV-1 infection of human fibroblasts occurs independently of type I IFN exposure (Alandijany *et al.*, 2018; Everett & Murray, 2005; Everett *et al*, 2004; Maul *et al.*, 1996), and we confirmed this was also the case in dermal fibroblasts isolated from postnatal mice (Fig. EV3A, B), Therefore, the presence of IFNα during initial infection can impact the long-term subnuclear localization of latent viral genomes in neurons by inducing PML-NBs that persist and stably entrap latent viral genomes.

Thus far, our data indicate that the presence of IFNα during initial infection determines subnuclear positioning of latent viral genomes and the ability of genomes to reactivate in response to inhibition of PI3 kinase activity. We considered that type I IFN treatment could have a long-term effect on cell signaling pathways which could impact the ability of HSV to reactivate. Therefore, to determine the direct versus indirect effects on the viral genome itself, we next investigated whether the timing of IFNα exposure had a differential effect on the ability of viral genomes to reactivate. We treated postnatal SCG neurons with IFNα (600 IU/ml) for 18h and during the 2h HSV inoculation (-18hpi) or exposed neurons to IFNα for 18h at 3 days prior to infection (-3dpi). Following pretreatment at -3dpi or -18hpi, IFNα was washed out and an IFNAR1 blocking antibody was used. As expected, IFNα during initial infection significantly inhibited HSV reactivation, but surprisingly, IFNα treatment at -3dpi did not restrict reactivation as shown by the similar number of GFP-positive neurons at 72 hours post-reactivation when compared to untreated neurons (Fig. 5A). Consistent with the reactivation data, we found that vDNA foci did not localize to PML-NBs in SCG neurons

390 treated with IFNα at -3dpi (Fig. 5B). We confirmed that PML-NBs were present at the
391 time of infection in neurons treated 3 day prior to infection (Fig. 5C), although we did
392 detect slightly fewer PML-NBs per nucleus in neurons treated -3dpi compared to -18hpi
393 (a mean of 17.57 versus 12.47 per nucleus respectively). We also confirmed
394 comparable recruitment of known PML-NB-associated proteins ATRX, Daxx and
395 SUMO-1 at 3 days post-IFNα treatment (Fig EV4A-5C). When IFNα treatment of SCG
396 neurons is continued from -3dpi through infection, or if SCG neurons treated at -3dpi
397 receive a second treatment of IFNα during infection, then a similar proportion of latent
398 viral genomes colocalize with PML-NBs as with a single treatment during infection (Fig.
399 EV4D). Together with the previous data on genome entrapment in dermal fibroblasts
400 (Fig. EV3A, B), these data indicate that type I IFN must be present during infection of
401 neurons, but not necessarily non-neuronal cells, for vDNA to colocalize with PML-NBs.
402
403 The HSV Infected Cell Protein 0 (ICP0) is a RING-finger E3 ubiquitin ligase that
404 is synthesized at very early stages of HSV-1 infection (Boutell *et al.*, 2002). During lytic
405 infection, it localizes to PML-NBs and disrupts their integrity by targeting PML and other
406 PML-NB associated proteins for degradation (Alandijany *et al.*, 2018; Boutell *et al*, 2011;
407 Boutell *et al.*, 2002; Chelbi-Alix & de The, 1999; Cuchet-Lourenco *et al*, 2012; Everett *et*
408 *al*, 1998; Muller *et al*, 1998). This activity is required for promoting the efficient onset of
409 HSV-1 lytic replication, and ICP0-null mutants exhibit a defect in viral gene expression
410 in certain cell types at low multiplicities of infection (Everett *et al*, 2008). ICP0 mRNA is
411 also known to be expressed during the establishment of latency (Cliffe *et al*, 2013).
412 Therefore, the colocalization of latent viral genomes to PML-NBs and ultimately the

ability of HSV to undergo reactivation could be due the presence of IFNα during initial infection and its effect on the localization or amount of ICP0. To investigate the distribution of ICP0 at early time points post-infection, SCG neurons were treated with IFNα at either -3dpi or -18hpi and infected at a MOI of 7.5 PFU/cell with HSV-1 Us11-GFP in the presence of acyclovir (ACV). In both treatment groups, ICP0 staining similarly colocalized with puncta of ATRX, a correlate for PML-NBs, at 3, 6 and 9 hours post-infection (Fig. EV4E, F). Interestingly, foci of ATRX still remained even with the presence of ICP0, suggesting that ICP0 is not disrupting the integrity of PML-NBs in this system. To further investigate the effect of ICP0 on the colocalization of latent viral genomes to PML-NBs, we generated an EdC-labeled ICP0-null mutant strain n212 (Cai & Schaffer, 1989) and rescue (Lee *et al*, 2016) verified by immunofluorescence (Fig EV4G) and found that the presence or absence of ICP0 had no detectable impact on the ability of vDNA foci to colocalize to PML-NBs (Fig. 5D). Taken together, these data demonstrate that association of latent viral genomes with PML-NBs in peripheral neurons is dependent on the formation of type I IFN-induced PML-NBs and the presence of type I IFN during initial infection and is independent of ICP0 expression.

PML is Required for the IFNα-dependent Restriction of HSV-1 Latency

To determine whether the stable association of viral genomes with PML-NBs directly contributes to the IFNα-dependent restriction of HSV reactivation, we investigated whether PML depletion was sufficient to restore the ability of the latent viral genomes to reactivate. A previous study has shown that PML-dependent recruitment of HIRA to ISG promoters contributes to the up-regulation of gene expression as a result

436 of cytokine release in response to HSV infection (McFarlane *et al.*, 2019). Although
437 carried out in non-neuronal cells, this study and others (Chen *et al*, 2015; Kim & Ahn,
438 2015; Scherer *et al*, 2016; Ulbricht *et al*, 2012) suggest that PML itself may contribute to
439 ISG upregulation, so to determine whether PML was indeed required for ISG stimulation
440 in SCG neurons we carried out RNA deep sequence analysis in IFNα-treated neurons
441 depleted of PML. Postnatal SCG neurons were transduced with lentiviral vectors
442 expressing non-targeting control or PML-targeting shRNAs (shCtrl and shPML,
443 respectively) and then mock treated or treated with IFNα (600 IU/ml) for 18h prior to
444 RNA extraction for next generation sequencing**.** High confidence reads were used for
445 gene expression and gene ontology (GO) analysis. As expected, treatment of shCtrl
446 transduced neurons with IFNα caused large changes in differentially regulated gene
447 expression, with an enrichment of upregulated genes involved in immune system
448 regulation. Similar to control neurons, PML depleted neurons also significantly
449 upregulated the expression of genes involved in the response to IFNα stimulation. We
450 found that of the total of 248 genes upregulated >1.5-fold following IFNα treatment,
451 83.47% of these genes were shared between the shCtrl- and shPML-treated groups
452 (Fig. EV5A). Furthermore, we found similar ISG expression (Fig. EV5B) and GO
453 pathway enrichment (Fig. EV5C). Therefore, in primary SCG neurons, the expression of
454 ISGs in response to exogenous IFNα is largely independent of PML expression.
455
456 Because PML depletion did not detectably prevent the induction of type I IFN
457 response genes in SCG neurons, we were able to examine the effect of PML depletion
458 prior to infection on the IFNα-mediated restriction of HSV-1 reactivation. SCG neurons

were transduced with lentiviral vectors expressing different PML-targeting shRNA or control non-targeting shRNA. PML depletion was confirmed by average number of PML-NBs per nucleus (Fig. 6A) and *Pml* mRNA expression level (Fig. EV5D, E) in neurons transduced for 3 days then treated with IFNα (600 IU/ml). As expected, we found a significant decrease in the percent of vDNA foci stably colocalizing with PML-NBs at 8 dpi in the shPML-treated neurons compared to shCtrl-treated neurons (Fig. 6B). Furthermore, we assessed reactivation in neurons infected with HSV-1 in the presence or absence of IFNα (150 IU/ml) at 3 days post-transduction. In these experiments, neurons were infected with a Us11-GFP gH-null virus, which is defective in cell-to-cell spread and eliminates the need for WAY-150138 during reactivation. In untreated neurons, we found no difference in reactivation following treatment with LY294002 (Fig. 6C, D). In addition, PML depletion had no effect on the number of GFP-positive neurons in the non-reactivated samples, indicating that in this system that PML was not required for the establishment of latency. However, in neurons treated with IFNα at the time of initial infection, depletion of PML using either of the three PML shRNAs increased the ability of HSV to reactivate as indicated by a 2.97-, 2.69- and 3.49- fold increase in GFP-positive neurons following treatment with LY294002, respectfully (Fig. 6E, F). Moreover, there was no significant difference between the PML depleted, IFNα-treated neurons and the non-IFNα treated neurons, indicating that PML depletion fully restored the ability of HSV to reactivate from type I IFN treated neurons. Taken together, these data demonstrate that type I IFN exposure solely at the time of infection results in entrapment of viral genomes in PML-NBs and restricts reactivation. This suggests that

genome entrapment by PML promotes a more restrictive or deeper form of latency where reactivation is limited.

Depletion of PML After the Establishment of Latency Enhances Reactivation in IFNα-treated Neurons

To explore the long-term effect of stable PML-NB-association on the latent viral genome, we next tested whether PML depletion after the establishment of latency was sufficient to restore the ability of the latent viral genomes to reactivate following treatment with a trigger that may directly disrupt PML-NBs. Arsenic trioxide (ATO) has been shown to bind directly to PML and disrupt PML-NBs (Lallemand-Breitenbach *et al*, 2008; Sides *et al*, 2011; Zhang *et al*, 2010), and we confirmed that ATO (1μM) fully disrupted IFNα-induced PML-NBs in our peripheral neurons by 18h post-treatment (Fig. EV5F). When we investigated reactivation in neurons that were latently infected in the presence or absence of IFNα, then treated with arsenic trioxide (ATO) at 8 dpi, we found that ATO is a very potent stimulator of reactivation independent of IFNα-treatment, indicating that ATO is capable of triggering reactivation of genomes that are either PML-NB-associated or not (Fig. EV5G). This is likely because ATO is a potent activator of the cell stress response and can result in robust histone phosphorylation (Gehani et al, 2010), which we have previously linked to reactivation (Cliffe et al., 2015). Although ATO could also induce reactivation in the presence of IFNα-induced PML-NBs, this reactivation was still less robust than mock treated neurons, likely reflecting the time required for disruption of PML-NBs by ATO.

Therefore, to more specifically determine whether PML-depletion restored the ability of neurons to reactivate following treatment with a physiological stimulus of

505 reactivation, Neurons were infected with Us11-GFP gH null HSV-1 virus in the presence
506 or absence of IFNα (150 IU/ml) and subsequently transduced with lentiviral vectors
507 expressing PML-targeting shRNA or control non-targeting shRNA at 1 dpi. Under these
508 experimental conditions, PML knockdown post-infection did not impact LY294002-
509 induced reactivation in untreated neurons (Fig. 7A, C), but did increase the ability of
510 HSV to reactivate from IFNα treated neurons in response to treatment with LY294002,
511 as indicated by a 1.3-fold increase in GFP-positive neurons, albeit reactivation was not
512 restored to levels seen in untreated neurons (Fig. 7B, D). As expected, we found that
513 only a small proportion of vDNA foci stably colocalize with PML-NBs at 8 dpi in the
514 shPML-treated neurons compared to vDNA foci in the shCtrl-treated neurons (Fig. 7E).
515 Therefore, PML depletion post-infection does not result in detectable spontaneous
516 reactivation of PML-NB-associated viral genomes, indicating that they are still in a
517 repressed state and/or lack the necessary factors required to initiate gene expression.
518 However, depletion of PML does partially restore the ability of HSV to enter the lytic
519 from IFN-treated neurons in response to a reactivation stimulus.
520
521 Previously we have shown that reactivation in response to LY294002 is
522 dependent on activation of the neuronal stress pathway involved dual-leucine zipper
523 kinase (DLK) and JNK activation (Cliffe *et al.*, 2015). To test whether the same cell
524 stress stimuli is required to induce reactivation from genomes released from PML-NBs
525 upon shRNA-mediated knockdown of PML, we reactivated in the presence of the DLK
526 inhibitor GNE-3511 (Patel *et al*, 2015). GNE-3511 inhibited LY294002-mediated
527 reactivation of latent genomes following PML depletion post-infection (Figure 7F).

Therefore, PML-NBs maintain a restricted form of latency that is more refractory to reactivation, and following PML depletion, viral genomes do not undergo detectable spontaneous reactivation and are still dependent on activation of neuronal cell stress signaling pathways for reactivation.

,

Discussion

The considerable heterogeneity observed at the neuronal level in the colocalization of viral genomes with different nuclear domains may reflect in different types of latency that are more or less susceptible to reactivation. The determinants of this heterogeneity and a direct link between the subnuclear localization of a latent genome and its ability to reactivate following a given stimulus was not known. Using a primary neuronal model of HSV latency and reactivation, we found that the presence of type I IFN solely at that time of initial infection acts as a key mediator of the subnuclear distribution of latent viral genomes in neurons and promotes a more restricted form of latency that is less capable of reactivation following disruption of NGF-signaling. Importantly, we show that activation of the type I IFN signaling pathway in peripheral neurons induces the detectable formation of PML-NBs, which stably entrap a proportion of latent genomes. Importantly, we show that this IFN-dependent restriction is mediated by PML, suggesting that PML-NBs are directly responsible for the observed restriction of reactivation.

PML-NBs typically number 1-30 bodies per nucleus in non-neuronal cells (Bernardi & Pandolfi, 2007). In the mouse nervous system, however, *Pml* mRNA expression levels have previously been found to be low as measured by *in situ* hybridization (Gray *et al*, 2004). PML protein is enriched in neural progenitor cells, but the induction of differentiation results in the downregulation of PML both at a transcriptional and protein level, and *P*ml mRNA expression is undetectable in post-mitotic neurons in many regions of the developing brain (Regad *et al*, 2009). Our

559 findings in postnatal peripheral neurons further support these observations. *Pml*
560 expression in adult mouse neurons varies considerably between brain regions but is
561 generally confined to the gray matter (Hall *et al*, 2016). Although implicated to play a
562 role in regulating circadian rhythms (Miki *et al*, 2012), synaptic plasticity (Bloomer *et al*,
563 2007) and the response to toxic proteins that cause neurodegenerative disorders (Chort
564 *et al*, 2013; Kumada *et al*, 2002; Mackenzie *et al*, 2006; Yamada *et al*, 2001), PML
565 regulation and function in adult nervous system is still largely unknown. In our study,
566 we could not detect PML-NBs in adult primary neurons isolated from the SCG or the
567 TG. In contrast to our findings, PML-NBs have previously been shown to be present in
568 adult mouse and human TG neurons by FISH and immunofluorescence (Catez *et al.*,
569 2012; Maroui *et al.*, 2016). However, no quantification was done in these studies, and
570 Catez *et al.* (2012) describes subpopulations of adult TG neurons that did not display
571 any PML signal in the nucleus. In addition, characterization of PML distribution in adult
572 TG neurons by IF-FISH of ganglia isolated *in vivo* may reflect prior exposure to type I
573 IFNs or other signaling molecules. The functional significance of peripheral neurons
574 lacking PML-NBs is unclear, but could be linked to the capacity of neurons to undergo
575 dynamic rearrangement of local and global nuclear architecture during maturation or
576 neuronal excitation. An absence of PML-NBs in neurons could also contribute to their
577 resistance to apoptosis, as PML has also been shown to play a role in cell death
578 through the induction of both p53-dependent and -independent apoptotic pathways
579 (Guo *et al*, 2000; Quignon *et al*, 1998; Wang *et al*, 1998). Whether PML-mediated
580 regulation of these pathways occurs in the context of PML-NBs or by PML itself is
581 unclear, but interestingly, the pro-apoptotic functions of Daxx, a PML-NB-associated

582 protein, may require localization to PML-NBs in certain cell types (Croxton *et al*, 2006).
583 Furthermore, our *in vitro* model using pure populations of intact neurons is devoid of the
584 immune responses and complexities of intact animals, and we cannot rule out the
585 possibility that axotomy or the processing of the neurons *ex vivo* could lead to PML-NB
586 disruption or dispersal. However, notwithstanding these caveats, primary neurons
587 provide an excellent model system to understand the impact of extrinsic immune factors
588 and PML-NBs to the altering the nature of HSV latency.
589
590 Peripheral neurons are capable of responding to type I IFN signaling, given the
591 robust induction in ISG expression and formation of PML-NBs following treatment with
592 IFNα, and this is supported by a number of previous studies (Barragan-Iglesias *et al*,
593 2020; Katzenell & Leib, 2016; Linderman *et al.*, 2017; Song *et al*, 2016; Yordy *et al*,
594 2012). Importantly, however, peripheral neurons produce little to no type I interferons
595 upon HSV infection (Rosato & Leib, 2014; Yordy *et al.*, 2012), indicating that IFN
596 production arises from other surrounding infected cells. Infected fibroblasts at the body
597 surface, as well as professional immune cells, have been shown to produce high levels
598 of IFNα/β after HSV infection (Hochrein *et al*, 2004; Li *et al*, 2006; Rasmussen *et al*,
599 2009; Rasmussen *et al*, 2007). In addition, there is evidence of elevated type I IFN in
600 peripheral ganglia during HSV-1 infection (Carr *et al.*, 1998), suggesting that glial or
601 immune cells located adjacent to peripheral neuron cell bodies are capable of type I IFN
602 production. It will be important to delineate if the inflammatory environment at the initial
603 site of infection acts on neuronal axons to prime the neuron for a more repressed latent
604 infection or if inflammatory cytokines in the ganglia are crucial for promoting a more

repressive state. Although responsive to IFN, primary peripheral and cortical mouse neurons have previously been shown to have inefficient type I IFN-mediated anti-viral protection compared to non-neuronal mitotic cells (Kreit *et al*, 2014; Yordy *et al.*, 2012). One study showed that DRG neurons are less responsive to type I IFN signaling and used an absence of cell death upon IFN treatment as one of their criteria (Yordy *et al.*, 2012). It should be noted that different cell types display specific responses to type I IFN signaling and peripheral neurons have even been reported to be more protected from cell death stimuli following IFN treatment (Chang *et al*, 1990). Furthermore, a previous study found that inducible reactivation of HSV-1 from latently infected neuronal cultures is transiently sensitive to type I IFNs (Linderman *et al.*, 2017). Our model of HSV-1 latency and reactivation in primary sympathetic neurons highlights a type I IFN response that is PML-dependent and suggests a role for neuronal IFN signaling in promoting a more restricted latent HSV-1 infection.

Prior to this study, it was not clear whether viral genomes associated with PML-NBs were capable of undergoing reactivation. In response to inhibition of NGF-signaling, our data demonstrate that PML-NB associated genomes are more restricted for reactivation given that 1) IFN induces PML-NB formation and increased association with viral genomes with PML-NBs, 2) IFN pretreatment promotes restriction of viral reactivation and 3) the ability of viral genomes to reactivate from IFN-treated neurons increases with PML knock-down either prior to or following infection. Previous work by Cohen *et al.* (2018) showed that quiescent genomes associated with PML-NBs in fibroblasts can be transcriptionally reactivated by induced expression of ICP0. However,

628 this previous study did not address the capability of viral genomes to reactivate in the
629 absence of viral lytic protein (i.e. during reactivation from latency in neurons). In a
630 further study using primary neurons, treatment of quiescently-infected neurons with the
631 histone deacetylase inhibitor, trichostatin A (TSA), could lead to disruption of PML-NBs
632 and induce active viral transcription in a subset of PML-NB-associated genomes
633 (Maroui *et al.*, 2016). However, the mechanisms of reactivation following TSA treatment
634 are not known, and may be direct via altering the HSV chromatin structure or indirect via
635 increasing the acetylation levels of histones or non-histone proteins, including PML.
636 How increased acetylation relates to the physiological triggers that induce HSV
637 reactivation is not clear. In contrast, loss of neurotrophic signaling can occur in
638 response to known physiological stimuli that trigger HSV reactivation (Suzich & Cliffe,
639 2018). Although we cannot rule out the possibility that different stimuli have the potential
640 for PML-NB associated genomes to undergo reactivation, this study clearly
641 demonstrates that at least one well characterized trigger of reactivation cannot
642 efficiently induce PML-NB associated genomes to undergo transcription.
643
644 Our results identify a persistence of PML-NBs, an IFN-mediated innate immune
645 response, that allows for long-term restriction of latent viral genomes in the absence of
646 continued ISG expression. Interestingly, type I IFN-induced PML-NBs persisted for up to
647 15 days post-treatment both in the presence and absence of viral infection. Given the
648 absence of PML-NBs in our untreated peripheral neurons, this induction and
649 persistence could represent neuron-specific innate immune memory. The persistence of
650 PML-NBs in neurons may alter the subsequent response to IFN and/or viral infection,

651 and it will be interesting to determine whether there is trained immunity in neurons such
652 that subsequent responses differ from the first exposure. What is clear from our results
653 however is the role of PML and IFN exposure in sustained repression of the latent HSV
654 genome. Even in the absence of known chromatin changes that occur on the PML
655 associated viral genome, this long-term effect on the ability of the HSV-1 genome to
656 respond to an exogenous signal and restriction of reactivation is reminiscence of the
657 classical definition of an epigenetic change (of course in the case of post-mitotic
658 neurons in the absence of inheritance).
659
660 Here we demonstrate that there are different types of HSV latency dependent on the
661 subnuclear positioning of the viral genome and ability to reactivate. Genomes
662 associated with PML-NBs are one form of restricted latency in our system. PML-NBs
663 are known to play a role in the restriction of viral gene expression in non-neuronal cells,
664 but the potential mechanism of PML-NB-mediated HSV gene silencing in neurons is
665 unknown. During latency, the viral genome is enriched with histone post-translational
666 modifications (PTMs) consistent with repressive heterochromatin, including H3K9me2/3
667 and H3K27me3, and it is possible that PML-NBs play a role in the association of viral
668 genomes with core histones, repressive PTMs or heterochromatin-associated proteins
669 (Cliffe *et al.*, 2009; Kwiatkowski *et al.*, 2009; Wang *et al.*, 2005), or instead via physical
670 compaction of the viral genome in PML-NBs. Although PML-NBs promote a more
671 restricted form of latency, we have shown that latency can be established in the
672 absence of IFN treatment and PML-NBs. Even in IFN-treated neurons, only a proportion
673 of the latent viral genomes co-localized with PML-NBs. This indicates that latent

genomes associate with other subnuclear regions and proteins that may promote the assembly and/or maintenance of repressive heterochromatic histone modifications. This supports previous observations that HSV-1 viral genomes also co-localize with centromeric repeats and other, undefined nuclear domains in latently infected TG *in vivo* (Catez *et al.*, 2012). For example, the viral genome is known to be enriched for H3K27me3 (Cliffe *et al.*, 2009; Kwiatkowski *et al.*, 2009; Wang *et al.*, 2005), which can be bound by Polycomb group proteins. Interestingly, we have found that the multi-functional, chromatin remodeler protein ATRX has abundant nuclear staining in neurons and, in contrast to non-neuronal cells, is localized outside of PML-NBs. ATRX staining overlapped with Hoechst DNA staining in our primary neurons, suggesting its localization with AT-rich heterochromatin regions (Bucevicius *et al*, 2019).Ultimately, the latent viral genomes are likely bound by ATRX, Polycomb group proteins or other repressive cellular proteins independently of PML-NBs. Investigating the identity, mechanism of targeting and role of these proteins in the induction and maintenance of latency will ultimately facilitate the development of antiviral therapeutics that target the latent stage of infection to prevent reactivation.

Materials and Methods

Reagents

Compounds used in the study are as follows: Acycloguanosine, FUDR, LY 294002, Nerve Growth Factor 2.5S (Alomone Labs), Primocin (Invivogen), Aphidicolin (AG Scientific), IFN-α (EMD Millipore IF009) , IFN-β (EMD Millipore IF011), IFN-γ (EMD Millipore IF005), IFN-λ2 (PeproTech 250-33); WAY-150138 was kindly provided by Pfizer, Dr. Jay Brown and Dr. Dan Engel at the University of Virginia, and Dr. Lynn Enquist at Princeton University. Compound information and concentrations used can be found below in Table S1.

Preparation of HSV-1 Virus Stocks

HSV-1 stocks of eGFP-Us11 Patton were grown and titrated on Vero cells obtained from the American Type Culture Collection (Manassas, VA). Cells were maintained in Dulbecco's Modified Eagle's Medium (Gibco) supplemented with 10% FetalPlex (Gemini Bio-Products) and 2 mM L-Glutamine. eGFP-Us11 Patton (HSV-1 Patton strain with eGFP reporter protein fused to true late protein Us11 (Benboudjema *et al*, 2003)) was kindly provided by Dr. Ian Mohr at New York University.

Stayput Us11-GFP was created by inserting an eUs11-GFP tag into the previously created gH-deficient HSV-1 SCgHZ virus (strain SC16) through co-transfection of SCgHZ viral DNA and pSXZY-eGFP-Us11 plasmid (Forrester *et al*, 1992). Stayput Us11-GFP is propagated and titrated on previously constructed Vero F6 cells, which contain copies of the gH gene under the control of an HSV-1 gD promoter, as described

720 in Forrester *et al.* (1992). Vero F6s are maintained in Dulbecco's Modified Eagle's
721 Medium (Gibco) supplemented with 10% FetaPlex (Gemini BioProducts). They are
722 selected with The supplementation of 250 ug/mL of G418/Geneticin (Gibco).
723
724 **Primary Neuronal Cultures**
725 Sympathetic neurons from the Superior Cervical Ganglia (SCG) of post-natal day 0-2
726 (P0-P2) or adult (P21-P24) CD1 Mice (Charles River Laboratories) were dissected as
727 previously described (Cliffe *et al.*, 2015). Sensory neurons from Trigeminal Ganglia (TG)
728 of post-natal day 0-2 (P0-P2) CD1 mice (Charles River Laboratories) were dissected
729 using the same protocol. Sensory neurons from TG of adult were dissected as
730 previously described (Bertke *et al*, 2011) with a modified purification protocol using
731 Percoll from the protocol published by Malin *et al* (2007). Rodent handling and
732 husbandry were carried out under animal protocols approved by the Animal Care and
733 Use Committee of the University of Virginia (UVA). Ganglia were briefly kept in
734 Leibovitz's L-15 media with 2.05 mM L-Glutamine before dissociation in Collagenase
735 Type IV (1 mg/mL) followed by Trypsin (2.5 mg/mL) for 20 minutes each at 37 ˚C.
736 Dissociated ganglia were triturated, and approximately 10,000 neurons per well were
737 plated onto rat tail collagen in a 24-well plate. Sympathetic neurons were maintained in
738 CM1 (Neurobasal® Medium supplemented with PRIME-XV IS21 Neuronal Supplement
739 (Irvine Scientific), 50 ng/mL Mouse NGF 2.5S, 2 mM L-Glutamine, and Primocin).
740 Aphidicolin (3.3 µg/mL) was added to the CM1 for the first five days post-dissection to
741 select against proliferating cells. Sensory neurons were maintained in the same media
742 supplemented with GDNF (50ng/ml; Peprotech 450-44)

Establishment and Reactivation of Latent HSV-1 Infection in Primary Neurons

Latent HSV-1 infection was established in P6-8 sympathetic neurons from SCGs. Neurons were cultured for at least 24 hours without antimitotic agents prior to infection. The cultures were infected with eGFP-Us11 (Patton recombinant strain of HSV-1 expressing an eGFP reporter fused to true late protein Us11) or StayPut. Neurons were infected at a Multiplicity of Infection (MOI) of 7.5 PFU/cell with eGFP-Us11 and at an MOI of 5 PFU/cell with StayPut (assuming $1.0x10^4$ neurons/well/24-well plate) in DPBS +$CaCl_2$ +$MgCl_2$ supplemented with 1% Fetal Bovine Serum, 4.5 g/L glucose, and 10 μM Acyclovir (ACV) for 2-3 hours at 37 ˚C. Post-infection, inoculum was replaced with CM1 containing 50 μM ACV and an anti-mouse IFNAR-1 antibody (Leinco Tech I-1188, 1:1000) for 5-6 days, followed by CM1 without ACV. Reactivation was carried out in DMEM/F12 (Gibco) supplemented with 10% Fetal Bovine Serum, Mouse NGF 2.5S (50 ng/mL) and Primocin. WAY-150138 (10 μg/mL) was added to reactivation cocktail to limit cell-to-cell spread. Reactivation was quantified by counting number of GFP-positive neurons or performing Reverse Transcription Quantitative PCR (RT-qPCR) of HSV-1 lytic mRNAs isolated from the cells in culture.

Analysis of mRNA expression by reverse-transcription quantitative PCR (RT-qPCR)

To assess relative expression of HSV-1 lytic mRNA, total RNA was extracted from approximately $1.0x10^4$ neurons using the Quick-RNA™ Miniprep Kit (Zymo Research) with an on-column DNase I digestion. mRNA was converted to cDNA using the

SuperScript IV First-Strand Synthesis system (Invitrogen) using random hexamers for first strand synthesis and equal amounts of RNA (20-30 ng/reaction). To assess viral DNA load, total DNA was extracted from approximately $1.0x10^4$ neurons using the Quick-DNA™ Miniprep Plus Kit (Zymo Research). qPCR was carried out using *Power* SYBR™ Green PCR Master Mix (Applied Biosystems). The relative mRNA or DNA copy number was determined using the Comparative C_T ($\Delta\Delta C_T$) method normalized to mRNA or DNA levels in latently infected samples. Viral RNAs were normalized to mouse reference gene GAPDH. All samples were run in duplicate on an Applied Biosystems™ QuantStudio™ 6 Flex Real-Time PCR System and the mean fold change compared to the reference gene calculated. Primers used are described in Table S2.

Immunofluorescence

Neurons were fixed for 15 minutes in 4% Formaldehyde and blocked in 5% Bovine Serum Albumin and 0.3% Triton X-100 and incubated overnight in primary antibody. Following primary antibody treatment, neurons were incubated for one hour in Alexa Fluor® 488-, 555-, and 647-conjugated secondary antibodies for multi-color imaging (Invitrogen). Nuclei were stained with Hoechst 33258 (Life Technologies). Unless indicated otherwise, z-stack images images of entire nuclei were acquired using an sCMOS charge-coupled device camera (pco.edge) mounted on a Nikon Eclipse Ti Inverted Epifluorescent microscope and processed into 2D projection images using the NIS-Elements software (Nikon) Extended Depth of Focus (EDF) plug-in. Images were further analyzed and processed using ImageJ.

Click Chemistry

For EdC-labeled HSV-1 virus infections, an MOI of 5 was used. EdC labelled virus was prepared using a previously described method (McFarlane *et al.*, 2019). Click chemistry was carried out a described previously (Alandijany *et al.*, 2018) with some modifications. Neurons were washed with CSK buffer (10 mM HEPES, 100 mM NaCl, 300 mM Sucrose, 3 mM $MgCl_2$, 5 mM EGTA) and simultaneously fixed and permeabilized for 10 minutes in 1.8% methonal-free formaldehyde (0.5% Triton X-100, 1% phenylmethylsulfonyl fluoride (PMSF)) in CSK buffer, then washed twice with PBS before continuing to the click chemistry reaction and immunostaining. Samples were blocked with 3% BSA for 30 minutes, followed by click chemistry using EdC-labelled HSV-1 DNA and the Click-iT EdU Alexa Flour 555 Imaging Kit (ThermoFisher Scientific, C10638) according to the manufacturer's instructions with AFDye 555 Picolyl Azide (Click Chemistry Tools, 1288). For immunostaining, samples were incubated overnight with primary antibodies in 3% BSA. Following primary antibody treatment, neurons were incubated for one hour in Alexa Fluor® 488- and 647-conjugated secondary antibodies for multi-color imaging (Invitrogen). Nuclei were stained with Hoechst 33258 (Life Technologies). Epifluorescence microscopy images were acquired at 60x using an sCMOS charge-coupled device camera (pco.edge) mounted on a Nikon Eclipse Ti Inverted Epifluorescent microscope using NIS-Elements software (Nikon). Images were analyzed and processed using ImageJ. Confocal microscopy images were acquired using a Zeiss LSM 880 confocal microscope using the 63x Plan-Apochromat oil immersion lens (numerical aperture 1.4) using 405 nm, 488 nm, 543 nm, and 633 nm laser lines. Zen black software (Zeiss) was used for image capture, generating cut mask

channels, and calculating weighted colocalization coefficients. Exported images were processed with minimal adjustment using Adobe Photoshop and assembled for presentation using Adobe Illustrator.

Preparation of Lentiviral Vectors

Lentiviruses expressing shRNA against PML (PML-1 TRCN0000229547, PML-2 TRCN0000229549, PML-3 TRCN0000314605), or a control lentivirus shRNA (Everett *et al.*, 2006) were prepared by co-transfection with psPAX2 and pCMV-VSV-G (Stewart *et al*, 2003) using the 293LTV packaging cell line (Cell Biolabs). Supernatant was harvested at 40- and 64-hours post-transfection. Sympathetic neurons were transduced overnight in neuronal media containing 8μg/ml protamine and 50μM ACV.

RNA Sequence Analysis

Reads were checked for quality using FASTQC (v0.11.8), trimmed using BBMAP (v3.8.16b), and aligned to the mouse genome with GENCODE (vM22) annotations using STAR (v2.7.1a). Transcripts per million calculations were performed by RSEM (v1.3.1), the results of which were imported into R (v4.0.2) and Bioconductor (v3.12) using tximport (v1.18.0). Significant genes were called using DESeq2, using fold change cutoffs and pvalue cutoffs of 0.5 and 0.05 respectively. Results were visualized using Heatplus (v2.36.0), PCAtools (v2.2.0), and UpSetR (v1.4.0). Functional enrichment was performed using GSEA and Metascape.

Statistical Analysis

Power analysis was used to determine the appropriate sample sizes for statistical analysis. All statistical analysis was performed using Prism V8.4. A Mann-Whitney test was used for all experiments where the group size was 2. All other experiments were analyzed using a one-way ANOVA with a Tukey's multiple comparison. Specific analyses are included in the figure legends. For all reactivation experiments measuring GFP expression, viral DNA, gene expression or DNA load, individual biological replicates were plotted (an individual well of primary neurons) and all experiments were repeated from pools of neurons from at least 3 litters.

Data Availability

The RNA-seq dataset generated and analysed in the current study is available at the NCBI Gene Expression omnibus (accession number GSE166738):

https://www.ncbi.nlm.nih.gov/geo/query/acc.cgi?acc=GSE166738

Acknowledgements

We thank Dr. Ian Mohr at New York University for the gift of the Us11-GFP virus and Gary Cohen at the University of Pennsylvania for SCgHZ. This work was supported by R21AI151340 (ARC), R01NS105630 (ARC), The Owens Family Foundation (ARC), NIH/NEI F30EY030397 (JBS), NIH/NIAID T32AI007046 (JBS and SRC), T32GM007267 (JBS), NIH/NIGMS T32GM008136 (SD) and MRC (https://mrc.ukri.org) MC_UU_12014/5 (CB).

Author Contributions

Jon B. Suzich – Conceptualization, formal analysis, investigation, methodology, validation, visualization, writing – original draft, writing – review & editing

Sean Cuddy – Investigation, validation

Hiam Baidas – Investigation

Sara Dochnal – Investigation, validation

Eugene Ke – Data curation, formal analysis, methodology, software

Austin Schinlever – Investigation

Aleksandra Babnis – Investigation

Chris Boutell – Resources, writing – review & editing

Anna R. Cliffe - Conceptualization, formal analysis, funding acquisition, investigation, validation, methodology, project administration, supervision, validation, visualization, writing – original draft, writing – review & editing

Conflict of Interest Statement

The authors declare that they have no conflict of interest

References

Alandijany T, Roberts APE, Conn KL, Loney C, McFarlane S, Orr A, Boutell C (2018) Distinct temporal roles for the promyelocytic leukaemia (PML) protein in the sequential regulation of intracellular host immunity to HSV-1 infection. *PLoS Pathogens* 14: e1006769-1006736

Baringer JR, Pisani P (1994) Herpes simplex virus genomes in human nervous system tissue analyzed by polymerase chain reaction. *Annals of neurology* 36: 823-829

Baringer JR, Swoveland P (1973) Recovery of herpes-simplex virus from human trigeminal ganglions. *The New England journal of medicine* 288: 648-650

Barragan-Iglesias P, Franco-Enzastiga U, Jeevakumar V, Shiers S, Wangzhou A, Granados-Soto V, Campbell ZT, Dussor G, Price TJ (2020) Type I Interferons Act Directly on Nociceptors to Produce Pain Sensitization: Implications for Viral Infection-Induced Pain. *J Neurosci* 40: 3517-3532

Benboudjema L, Mulvey M, Gao Y, Pimplikar SW, Mohr I (2003) Association of the herpes simplex virus type 1 Us11 gene product with the cellular kinesin light-chain-related protein PAT1 results in the redistribution of both polypeptides. *J Virol* 77: 9192-9203

Bernardi R, Pandolfi PP (2007) Structure, dynamics and functions of promyelocytic leukaemia nuclear bodies. *Nat Rev Mol Cell Biol* 8: 1006-1016

Bertke AS, Swanson SM, Chen J, Imai Y, Kinchington PR, Margolis TP (2011) A5-positive primary sensory neurons are nonpermissive for productive infection with herpes simplex virus 1 in vitro. *J Virol* 85: 6669-6677

Bishop CL, Ramalho M, Nadkarni N, May Kong W, Higgins CF, Krauzewicz N (2006) Role for centromeric heterochromatin and PML nuclear bodies in the cellular response to foreign DNA. *Mol Cell Biol* 26: 2583-2594

Bloomer WA, VanDongen HM, VanDongen AM (2007) Activity-regulated cytoskeleton-associated protein Arc/Arg3.1 binds to spectrin and associates with nuclear promyelocytic leukemia (PML) bodies. *Brain Res* 1153: 20-33

Boutell C, Cuchet-Lourenco D, Vanni E, Orr A, Glass M, McFarlane S, Everett RD (2011) A viral ubiquitin ligase has substrate preferential SUMO targeted ubiquitin ligase activity that counteracts intrinsic antiviral defence. *PLoS Pathog* 7: e1002245

Boutell C, Sadis S, Everett RD (2002) Herpes simplex virus type 1 immediate-early protein ICP0 and is isolated RING finger domain act as ubiquitin E3 ligases in vitro. *J Virol* 76: 841-850

Bucevicius J, Keller-Findeisen J, Gilat T, Hell SW, Lukinavicius G (2019) Rhodamine-Hoechst positional isomers for highly efficient staining of heterochromatin. *Chem Sci* 10: 1962-1970

Cabral JM, Oh HS, Knipe DM (2018) ATRX promotes maintenance of herpes simplex virus heterochromatin during chromatin stress. *Elife* 7

Cai WZ, Schaffer PA (1989) Herpes simplex virus type 1 ICP0 plays a critical role in the de novo synthesis of infectious virus following transfection of viral DNA. *J Virol* 63: 4579-4589

Camarena V, Kobayashi M, Kim JY, Roehm P, Perez R, Gardner J, Wilson AC, Mohr I, Chao MV (2010) Nature and duration of growth factor signaling through receptor tyrosine kinases regulates HSV-1 latency in neurons. *Cell Host Microbe* 8: 320-330

Carr DJ, Veress LA, Noisakran S, Campbell IL (1998) Astrocyte-targeted expression of IFN-alpha1 protects mice from acute ocular herpes simplex virus type 1 infection. *J Immunol* 161: 4859-4865

Catez F, Picard C, Held K, Gross S, Rousseau A, Theil D, Sawtell N, Labetoulle M, Lomonte P (2012) HSV-1 genome subnuclear positioning and associations with host-cell PML-NBs and

centromeres regulate LAT locus transcription during latency in neurons. *PLoS Pathog* 8: e1002852
Chang JY, Martin DP, Johnson EM, Jr. (1990) Interferon suppresses sympathetic neuronal cell death caused by nerve growth factor deprivation. *J Neurochem* 55: 436-445
Chelbi-Alix MK, de The H (1999) Herpes virus induced proteasome-dependent degradation of the nuclear bodies-associated PML and Sp100 proteins. *Oncogene* 18: 935-941
Chelbi-Alix MK, Pelicano L, Quignon F, Koken MH, Venturini L, Stadler M, Pavlovic J, Degos L, de The H (1995) Induction of the PML protein by interferons in normal and APL cells. *Leukemia* 9: 2027-2033
Chen SH, Kramer MF, Schaffer PA, Coen DM (1997) A viral function represses accumulation of transcripts from productive-cycle genes in mouse ganglia latently infected with herpes simplex virus. *Journal of Virology* 71: 5878-5884
Chen Y, Wright J, Meng X, Leppard KN (2015) Promyelocytic Leukemia Protein Isoform II Promotes Transcription Factor Recruitment To Activate Interferon Beta and Interferon-Responsive Gene Expression. *Mol Cell Biol* 35: 1660-1672
Chort A, Alves S, Marinello M, Dufresnois B, Dornbierer JG, Tesson C, Latouche M, Baker DP, Barkats M, El Hachimi KH *et al* (2013) Interferon beta induces clearance of mutant ataxin 7 and improves locomotion in SCA7 knock-in mice. *Brain* 136: 1732-1745
Cliffe AR, Arbuckle JH, Vogel JL, Geden MJ, Rothbart SB, Cusack CL, Strahl BD, Kristie TM, Deshmukh M (2015) Neuronal Stress Pathway Mediating a Histone Methyl/Phospho Switch Is Required for Herpes Simplex Virus Reactivation. *Cell Host Microbe* 18: 649-658
Cliffe AR, Coen DM, Knipe DM (2013) Kinetics of facultative heterochromatin and polycomb group protein association with the herpes simplex viral genome during establishment of latent infection. *MBio* 4: e00590-00512-e00590-00512
Cliffe AR, Garber DA, Knipe DM (2009) Transcription of the herpes simplex virus latency-associated transcript promotes the formation of facultative heterochromatin on lytic promoters. *J Virol* 83: 8182-8190
Cliffe AR, Knipe DM (2008) Herpes simplex virus ICP0 promotes both histone removal and acetylation on viral DNA during lytic infection. *J Virol* 82: 12030-12038
Cliffe AR, Wilson AC (2017) Restarting Lytic Gene Transcription at the Onset of Herpes Simplex Virus Reactivation. *J Virol* 91: e01419-01416-01416
Clynes D, Higgs DR, Gibbons RJ (2013) The chromatin remodeller ATRX: a repeat offender in human disease. *Trends in Biochemical Sciences* 38: 461-466
Cohen C, Corpet A, Roubille S, Maroui MA, Poccardi N, Rousseau A, Kleijwegt C, Binda O, Texier P, Sawtell N *et al* (2018) Promyelocytic leukemia (PML) nuclear bodies (NBs) induce latent/quiescent HSV-1 genomes chromatinization through a PML NB/Histone H3.3/H3.3 Chaperone Axis. *PLoS Pathog* 14: e1007313
Croxton R, Puto LA, de Belle I, Thomas M, Torii S, Hanaii F, Cuddy M, Reed JC (2006) Daxx represses expression of a subset of antiapoptotic genes regulated by nuclear factor-kappaB. *Cancer Res* 66: 9026-9035
Cuchet-Lourenco D, Vanni E, Glass M, Orr A, Everett RD (2012) Herpes simplex virus 1 ubiquitin ligase ICP0 interacts with PML isoform I and induces its SUMO-independent degradation. *J Virol* 86: 11209-11222
Cuddy SR, Schinlever AR, Dochnal S, Seegren PV, Suzich J, Kundu P, Downs TK, Farah M, Desai BN, Boutell C *et al* (2020) Neuronal hyperexcitability is a DLK-dependent trigger of herpes simplex virus reactivation that can be induced by IL-1. *Elife* 9

Du T, Zhou G, Roizman B (2011) HSV-1 gene expression from reactivated ganglia is disordered and concurrent with suppression of latency-associated transcript and miRNAs. *Proceedings of the National Academy of Sciences* 108: 18820-18824

Efstathiou S, Preston CM (2005) Towards an understanding of the molecular basis of herpes simplex virus latency. *Virus Res* 111: 108-119

Everett RD, Chelbi-Alix MK (2007) PML and PML nuclear bodies: implications in antiviral defence. *Biochimie* 89: 819-830

Everett RD, Freemont P, Saitoh H, Dasso M, Orr A, Kathoria M, Parkinson J (1998) The disruption of ND10 during herpes simplex virus infection correlates with the Vmw110- and proteasome-dependent loss of several PML isoforms. *J Virol* 72: 6581-6591

Everett RD, Maul GG (1994) HSV-1 IE protein Vmw110 causes redistribution of PML. *EMBO J* 13: 5062-5069

Everett RD, Murray J (2005) ND10 components relocate to sites associated with herpes simplex virus type 1 nucleoprotein complexes during virus infection. *J Virol* 79: 5078-5089

Everett RD, Murray J, Orr A, Preston CM (2007) Herpes simplex virus type 1 genomes are associated with ND10 nuclear substructures in quiescently infected human fibroblasts. *J Virol* 81: 10991-11004

Everett RD, Parada C, Gripon P, Sirma H, Orr A (2008) Replication of ICP0-null mutant herpes simplex virus type 1 is restricted by both PML and Sp100. *J Virol* 82: 2661-2672

Everett RD, Rechter S, Papior P, Tavalai N, Stamminger T, Orr A (2006) PML contributes to a cellular mechanism of repression of herpes simplex virus type 1 infection that is inactivated by ICP0. *J Virol* 80: 7995-8005

Everett RD, Sourvinos G, Leiper C, Clements JB, Orr A (2004) Formation of nuclear foci of the herpes simplex virus type 1 regulatory protein ICP4 at early times of infection: localization, dynamics, recruitment of ICP27, and evidence for the de novo induction of ND10-like complexes. *J Virol* 78: 1903-1917

Forrester A, Farrell H, Wilkinson G, Kaye J, Davis-Poynter N, Minson T (1992) Construction and properties of a mutant of herpes simplex virus type 1 with glycoprotein H coding sequences deleted. *Journal of Virology* 66: 341-348

Garber DA, Schaffer PA, Knipe DM (1997) A LAT-associated function reduces productive-cycle gene expression during acute infection of murine sensory neurons with herpes simplex virus type 1. *Journal of Virology* 71: 5885-5893

Garrick D, Samara V, McDowell TL, Smith AJ, Dobbie L, Higgs DR, Gibbons RJ (2004) A conserved truncated isoform of the ATR-X syndrome protein lacking the SWI/SNF-homology domain. *Gene* 326: 23-34

Gehani SS, Agrawal-Singh S, Dietrich N, Christophersen NS, Helin K, Hansen K (2010) Polycomb Group Protein Displacement and Gene Activation through MSK-Dependent H3K27me3S28 Phosphorylation. *Molecular Cell* 39: 886-900

Gordon YJ, Romanowski EG, Araullo-Cruz T, Kinchington PR (1995) The proportion of trigeminal ganglionic neurons expressing herpes simplex virus type 1 latency-associated transcripts correlates to reactivation in the New Zealand rabbit ocular model. *Graefes Arch Clin Exp Ophthalmol* 233: 649-654

Gray PA, Fu H, Luo P, Zhao Q, Yu J, Ferrari A, Tenzen T, Yuk DI, Tsung EF, Cai Z *et al* (2004) Mouse brain organization revealed through direct genome-scale TF expression analysis. *Science* 306: 2255-2257

Greger JG, Katz RA, Ishov AM, Maul GG, Skalka AM (2005) The cellular protein daxx interacts with avian sarcoma virus integrase and viral DNA to repress viral transcription. *J Virol* 79: 4610-4618

Grotzinger T, Jensen K, Will H (1996) The interferon (IFN)-stimulated gene Sp100 promoter contains an IFN-gamma activation site and an imperfect IFN-stimulated response element which mediate type I IFN inducibility. *J Biol Chem* 271: 25253-25260

Guo A, Salomoni P, Luo J, Shih A, Zhong S, Gu W, Pandolfi PP (2000) The function of PML in p53-dependent apoptosis. *Nat Cell Biol* 2: 730-736

Hall MH, Magalska A, Malinowska M, Ruszczycki B, Czaban I, Patel S, Ambrozek-Latecka M, Zolocinska E, Broszkiewicz H, Parobczak K *et al* (2016) Localization and regulation of PML bodies in the adult mouse brain. *Brain Struct Funct* 221: 2511-2525

Hendricks RL, Weber PC, Taylor JL, Koumbis A, Tumpey TM, Glorioso JC (1991) Endogenously produced interferon alpha protects mice from herpes simplex virus type 1 corneal disease. *J Gen Virol* 72 (Pt 7): 1601-1610

Hill JM, Sedarati F, Javier RT, Wagner EK, Stevens JG (1990) Herpes simplex virus latent phase transcription facilitates in vivo reactivation. *Virology* 174: 117-125

Hochrein H, Schlatter B, O'Keeffe M, Wagner C, Schmitz F, Schiemann M, Bauer S, Suter M, Wagner H (2004) Herpes simplex virus type-1 induces IFN-alpha production via Toll-like receptor 9-dependent and -independent pathways. *Proc Natl Acad Sci U S A* 101: 11416-11421

Ives AM, Bertke AS (2017) Stress Hormones Epinephrine and Corticosterone Selectively Modulate Herpes Simplex Virus 1 (HSV-1) and HSV-2 Productive Infections in Adult Sympathetic, but Not Sensory, Neurons. *Journal of Virology* 91: e00582-00517-00512

Jones CA, Fernandez M, Herc K, Bosnjak L, Miranda-Saksena M, Boadle RA, Cunningham A (2003) Herpes simplex virus type 2 induces rapid cell death and functional impairment of murine dendritic cells in vitro. *J Virol* 77: 11139-11149

Kamada R, Yang W, Zhang Y, Patel MC, Yang Y, Ouda R, Dey A, Wakabayashi Y, Sakaguchi K, Fujita T *et al* (2018) Interferon stimulation creates chromatin marks and establishes transcriptional memory. *Proceedings of the National Academy of Sciences* 115: E9162-E9171

Katzenell S, Leib DA (2016) Herpes Simplex Virus and Interferon Signaling Induce Novel Autophagic Clusters in Sensory Neurons. *J Virol* 90: 4706-4719

Kim JY, Mandarino A, Chao MV, Mohr I, Wilson AC (2012) Transient reversal of episome silencing precedes VP16-dependent transcription during reactivation of latent HSV-1 in neurons. *PLoS Pathog* 8: e1002540

Kim YE, Ahn JH (2015) Positive role of promyelocytic leukemia protein in type I interferon response and its regulation by human cytomegalovirus. *PLoS Pathog* 11: e1004785

Knipe DM, Cliffe A (2008) Chromatin control of herpes simplex virus lytic and latent infection. *Nat Rev Microbiol* 6: 211-221

Kobayashi M, Wilson AC, Chao MV, Mohr I (2012) Control of viral latency in neurons by axonal mTOR signaling and the 4E-BP translation repressor. *Genes Dev* 26: 1527-1532

Kramer MF, Coen DM (1995) Quantification of transcripts from the ICP4 and thymidine kinase genes in mouse ganglia latently infected with herpes simplex virus. *J Virol* 69: 1389-1399

Kreit M, Paul S, Knoops L, De Cock A, Sorgeloos F, Michiels T (2014) Inefficient type I interferon-mediated antiviral protection of primary mouse neurons is associated with the lack of apolipoprotein l9 expression. *J Virol* 88: 3874-3884

Kumada S, Uchihara T, Hayashi M, Nakamura A, Kikuchi E, Mizutani T, Oda M (2002) Promyelocytic leukemia protein is redistributed during the formation of intranuclear inclusions

independent of polyglutamine expansion: an immunohistochemical study on Marinesco bodies. *J Neuropathol Exp Neurol* 61: 984-991
Kwiatkowski DL, Thompson HW, Bloom DC (2009) The polycomb group protein Bmi1 binds to the herpes simplex virus 1 latent genome and maintains repressive histone marks during latency. *J Virol* 83: 8173-8181
Lallemand-Breitenbach V, de The H (2010) PML nuclear bodies. *Cold Spring Harb Perspect Biol* 2: a000661
Lallemand-Breitenbach V, Jeanne M, Benhenda S, Nasr R, Lei M, Peres L, Zhou J, Zhu J, Raught B, de The H (2008) Arsenic degrades PML or PML-RARalpha through a SUMO-triggered RNF4/ubiquitin-mediated pathway. *Nat Cell Biol* 10: 547-555
Lee JS, Raja P, Knipe DM (2016) Herpesviral ICP0 Protein Promotes Two Waves of Heterochromatin Removal on an Early Viral Promoter during Lytic Infection. *mBio* 7: e02007-02015
Leib DA, Bogard CL, Kosz-Vnenchak M, Hicks KA, Coen DM, Knipe DM, Schaffer PA (1989) A deletion mutant of the latency-associated transcript of herpes simplex virus type 1 reactivates from the latent state with reduced frequency. *Journal of Virology* 63: 2893-2900
Lewis PW, Elsaesser SJ, Noh K-M, Stadler SC, Allis CD (2010) Daxx is an H3.3-specific histone chaperone and cooperates with ATRX in replication-independent chromatin assembly at telomeres. *Proceedings of the National Academy of Sciences of the United States of America* 107: 14075-14080
Li H, Zhang J, Kumar A, Zheng M, Atherton SS, Yu FS (2006) Herpes simplex virus 1 infection induces the expression of proinflammatory cytokines, interferons and TLR7 in human corneal epithelial cells. *Immunology* 117: 167-176
Linderman JA, Kobayashi M, Rayannavar V, Fak JJ, Darnell RB, Chao MV, Wilson AC, Mohr I (2017) Immune Escape via a Transient Gene Expression Program Enables Productive Replication of a Latent Pathogen. *Cell Rep* 18: 1312-1323
Lukashchuk V, Everett RD (2010) Regulation of ICP0-null mutant herpes simplex virus type 1 infection by ND10 components ATRX and hDaxx. *J Virol* 84: 4026-4040
Ma JZ, Russell TA, Spelman T, Carbone FR, Tscharke DC (2014) Lytic Gene Expression Is Frequent in HSV-1 Latent Infection and Correlates with the Engagement of a Cell-Intrinsic Transcriptional Response. *PLoS Pathogens* 10: e1004237
Mackenzie IR, Baker M, West G, Woulfe J, Qadi N, Gass J, Cannon A, Adamson J, Feldman H, Lindholm C *et al* (2006) A family with tau-negative frontotemporal dementia and neuronal intranuclear inclusions linked to chromosome 17. *Brain* 129: 853-867
Malin SA, Davis BM, Molliver DC (2007) Production of dissociated sensory neuron cultures and considerations for their use in studying neuronal function and plasticity. *Nat Protoc* 2: 152-160
Maroui MA, Callé A, Cohen C, Streichenberger N, Texier P, Takissian J, Rousseau A, Poccardi N, Welsch J, Corpet A *et al* (2016) Latency Entry of Herpes Simplex Virus 1 Is Determined by the Interaction of Its Genome with the Nuclear Environment. *PLoS Pathogens* 12: e1005834-1005828
Maul GG (1998) Nuclear domain 10, the site of DNA virus transcription and replication. *Bioessays* 20: 660-667
Maul GG, Ishov AM, Everett RD (1996) Nuclear domain 10 as preexisting potential replication start sites of herpes simplex virus type-1. *Virology* 217: 67-75

McFarlane S, Orr A, Roberts APE, Conn KL, Iliev V, Loney C, da Silva Filipe A, Smollett K, Gu Q, Robertson N *et al* (2019) The histone chaperone HIRA promotes the induction of host innate immune defences in response to HSV-1 infection. *PLOS Pathogens* 15: e1007667

Miki T, Xu Z, Chen-Goodspeed M, Liu M, Van Oort-Jansen A, Rea MA, Zhao Z, Lee CC, Chang KS (2012) PML regulates PER2 nuclear localization and circadian function. *EMBO J* 31: 1427-1439

Mikloska Z, Cunningham AL (2001) Alpha and gamma interferons inhibit herpes simplex virus type 1 infection and spread in epidermal cells after axonal transmission. *J Virol* 75: 11821-11826

Mikloska Z, Danis VA, Adams S, Lloyd AR, Adrian DL, Cunningham AL (1998) In vivo production of cytokines and beta (C-C) chemokines in human recurrent herpes simplex lesions--do herpes simplex virus-infected keratinocytes contribute to their production? *J Infect Dis* 177: 827-838

Moorlag S, Roring RJ, Joosten LAB, Netea MG (2018) The role of the interleukin-1 family in trained immunity. *Immunol Rev* 281: 28-39

Muller S, Matunis MJ, Dejean A (1998) Conjugation with the ubiquitin-related modifier SUMO-1 regulates the partitioning of PML within the nucleus. *EMBO J* 17: 61-70

Nicoll MP, Hann W, Shivkumar M, Harman LE, Connor V, Coleman HM, Proenca JT, Efstathiou S (2016) The HSV-1 Latency-Associated Transcript Functions to Repress Latent Phase Lytic Gene Expression and Suppress Virus Reactivation from Latently Infected Neurons. *PLoS Pathog* 12: e1005539

Noh KM, Maze I, Zhao D, Xiang B, Wenderski W, Lewis PW, Shen L, Li H, Allis CD (2015) ATRX tolerates activity-dependent histone H3 methyl/phos switching to maintain repetitive element silencing in neurons. *Proc Natl Acad Sci U S A* 112: 6820-6827

Patel S, Cohen F, Dean BJ, De La Torre K, Deshmukh G, Estrada AA, Ghosh AS, Gibbons P, Gustafson A, Huestis MP *et al* (2015) Discovery of dual leucine zipper kinase (DLK, MAP3K12) inhibitors with activity in neurodegeneration models. *J Med Chem* 58: 401-418

Perng GC, Jones C, Ciacci-Zanella J, Stone M, Henderson G, Yukht A, Slanina SM, Hofman FM, Ghiasi H, Nesburn AB *et al* (2000) Virus-induced neuronal apoptosis blocked by the herpes simplex virus latency-associated transcript. *Science* 287: 1500-1503

Proenca JT, Coleman HM, Connor V, Winton DJ, Efstathiou S (2008) A historical analysis of herpes simplex virus promoter activation in vivo reveals distinct populations of latently infected neurones. *Journal of General Virology* 89: 2965-2974

Quignon F, De Bels F, Koken M, Feunteun J, Ameisen JC, de The H (1998) PML induces a novel caspase-independent death process. *Nat Genet* 20: 259-265

Rasmussen SB, Jensen SB, Nielsen C, Quartin E, Kato H, Chen ZJ, Silverman RH, Akira S, Paludan SR (2009) Herpes simplex virus infection is sensed by both Toll-like receptors and retinoic acid-inducible gene- like receptors, which synergize to induce type I interferon production. *J Gen Virol* 90: 74-78

Rasmussen SB, Sorensen LN, Malmgaard L, Ank N, Baines JD, Chen ZJ, Paludan SR (2007) Type I interferon production during herpes simplex virus infection is controlled by cell-type-specific viral recognition through Toll-like receptor 9, the mitochondrial antiviral signaling protein pathway, and novel recognition systems. *J Virol* 81: 13315-13324

Regad T, Bellodi C, Nicotera P, Salomoni P (2009) The tumor suppressor Pml regulates cell fate in the developing neocortex. *Nat Neurosci* 12: 132-140

Richter ER, Dias JK, Gilbert II JE, Atherton SS (2009) Distribution of Herpes Simplex Virus Type 1 and Varicella Zoster Virus in Ganglia of the Human Head and Neck. *The Journal of infectious diseases* 200: 1901-1906

Rosato PC, Leib DA (2014) Intrinsic innate immunity fails to control herpes simplex virus and vesicular stomatitis virus replication in sensory neurons and fibroblasts. *J Virol* 88: 9991-10001

Sainz B, Jr., Halford WP (2002) Alpha/Beta interferon and gamma interferon synergize to inhibit the replication of herpes simplex virus type 1. *J Virol* 76: 11541-11550

Sawtell NM (1997) Comprehensive quantification of herpes simplex virus latency at the single-cell level. *J Virol* 71: 5423-5431

Scherer M, Otto V, Stump JD, Klingl S, Muller R, Reuter N, Muller YA, Sticht H, Stamminger T (2016) Characterization of Recombinant Human Cytomegaloviruses Encoding IE1 Mutants L174P and 1-382 Reveals that Viral Targeting of PML Bodies Perturbs both Intrinsic and Innate Immune Responses. *J Virol* 90: 1190-1205

Shalginskikh N, Poleshko A, Skalka AM, Katz RA (2013) Retroviral DNA methylation and epigenetic repression are mediated by the antiviral host protein Daxx. *J Virol* 87: 2137-2150

Sides MD, Block GJ, Shan B, Esteves KC, Lin Z, Flemington EK, Lasky JA (2011) Arsenic mediated disruption of promyelocytic leukemia protein nuclear bodies induces ganciclovir susceptibility in Epstein-Barr positive epithelial cells. *Virology* 416: 86-97

Song R, Koyuncu OO, Greco TM, Diner BA, Cristea IM, Enquist LW (2016) Two Modes of the Axonal Interferon Response Limit Alphaherpesvirus Neuroinvasion. *mBio* 7: e02145-02115

Stadler M, Chelbi-Alix MK, Koken MH, Venturini L, Lee C, Saib A, Quignon F, Pelicano L, Guillemin MC, Schindler C *et al* (1995) Transcriptional induction of the PML growth suppressor gene by interferons is mediated through an ISRE and a GAS element. *Oncogene* 11: 2565-2573

Stevens JG, Wagner EK, Devi-Rao GB, Cook ML, Feldman LT (1987) RNA complementary to a herpesvirus alpha gene mRNA is prominent in latently infected neurons. *Science* 235: 1056-1059

Stewart SA, Dykxhoorn DM, Palliser D, Mizuno H, Yu EY, An DS, Sabatini DM, Chen IS, Hahn WC, Sharp PA *et al* (2003) Lentivirus-delivered stable gene silencing by RNAi in primary cells. *Rna* 9: 493-501

Suzich JB, Cliffe AR (2018) Strength in diversity: Understanding the pathways to herpes simplex virus reactivation. *Virology* 522: 81-91

Thompson RL, Sawtell NM (1997) The herpes simplex virus type 1 latency-associated transcript gene regulates the establishment of latency. *J Virol* 71: 5432-5440

Thompson RL, Sawtell NM (2001) Herpes simplex virus type 1 latency-associated transcript gene promotes neuronal survival. *J Virol* 75: 6660-6675

Trousdale MD, Steiner I, Spivack JG, Deshmane SL, Brown SM, MacLean AR, Subak-Sharpe JH, Fraser NW (1991) In vivo and in vitro reactivation impairment of a herpes simplex virus type 1 latency-associated transcript variant in a rabbit eye model. *Journal of Virology* 65: 6989-6993

Ulbricht T, Alzrigat M, Horch A, Reuter N, von Mikecz A, Steimle V, Schmitt E, Kramer OH, Stamminger T, Hemmerich P (2012) PML promotes MHC class II gene expression by stabilizing the class II transactivator. *J Cell Biol* 199: 49-63

van Zeijl M, Fairhurst J, Jones TR, Vernon SK, Morin J, LaRocque J, Feld B, O'Hara B, Bloom JD, Johann SV (2000) Novel class of thiourea compounds that inhibit herpes simplex virus type 1 DNA cleavage and encapsidation: resistance maps to the UL6 gene. *J Virol* 74: 9054-9061

Wang J, Shiels C, Sasieni P, Wu PJ, Islam SA, Freemont PS, Sheer D (2004) Promyelocytic leukemia nuclear bodies associate with transcriptionally active genomic regions. *J Cell Biol* 164: 515-526

Wang Q-Y, Zhou C, Johnson KE, Colgrove RC, Coen DM, Knipe DM (2005) Herpesviral latency-associated transcript gene promotes assembly of heterochromatin on viral lytic-gene promoters in latent infection. *Proceedings of the National Academy of Sciences* 102: 16055-16059

Wang ZG, Ruggero D, Ronchetti S, Zhong S, Gaboli M, Rivi R, Pandolfi PP (1998) PML is essential for multiple apoptotic pathways. *Nat Genet* 20: 266-272

Warren KG, Brown SM, Wroblewska Z, Gilden D, Koprowski H, Subak-Sharpe J (1978) Isolation of latent herpes simplex virus from the superior cervical and vagus ganglions of human beings. *The New England journal of medicine* 298: 1068-1069

Wilcox CL, Johnson EM (1987) Nerve growth factor deprivation results in the reactivation of latent herpes simplex virus in vitro. *Journal of Virology* 61: 2311-2315

Wilcox CL, Smith RL, Freed CR, Johnson EM (1990) Nerve growth factor-dependence of herpes simplex virus latency in peripheral sympathetic and sensory neurons in vitro. *Journal of Neuroscience* 10: 1268-1275

Xu P, Roizman B (2017) The SP100 component of ND10 enhances accumulation of PML and suppresses replication and the assembly of HSV replication compartments. *Proc Natl Acad Sci U S A* 114: E3823-E3829

Yamada M, Sato T, Shimohata T, Hayashi S, Igarashi S, Tsuji S, Takahashi H (2001) Interaction between neuronal intranuclear inclusions and promyelocytic leukemia protein nuclear and coiled bodies in CAG repeat diseases. *Am J Pathol* 159: 1785-1795

Yordy B, Iijima N, Huttner A, Leib D, Iwasaki A (2012) A neuron-specific role for autophagy in antiviral defense against herpes simplex virus. *Cell Host and Microbe* 12: 334-345

Zhang XW, Yan XJ, Zhou ZR, Yang FF, Wu ZY, Sun HB, Liang WX, Song AX, Lallemand-Breitenbach V, Jeanne M *et al* (2010) Arsenic trioxide controls the fate of the PML-RARalpha oncoprotein by directly binding PML. *Science* 328: 240-243

Zhong S, Muller S, Ronchetti S, Freemont PS, Dejean A, Pandolfi PP (2000a) Role of SUMO-1-modified PML in nuclear body formation. *Blood* 95: 2748-2752

Zhong S, Salomoni P, Pandolfi PP (2000b) The transcriptional role of PML and the nuclear body. *Nat Cell Biol* 2: E85-90

Figure Legends

Fig. 1. Type I IFN induces the formation of PML-NBs in primary peripheral neurons.

(**A**) Representative images of primary neurons isolated from superior cervical ganglia (SCG) and sensory trigeminal ganglia (TG) of postnatal (P6) and adult (P28) mice stained for PML and the neuronal marker BIII-tubulin.

(**B**) SCG and TG neurons isolated from P6 and P28 mice were treated with interferon (IFN)α (600 IU/ml) for 18h and stained for PML and BIII-tubulin.

(**C-F**) Quantification of detectable PML puncta in P6 and P28 neurons following 18h treatment with IFNα (150 IU/ml, 600 IU/ml), IFNγ (150 IU/ml, 500 IU/ml) and IFNλ2 (100 ng/ml, 500 ng/ml).

Data information: Data represent the mean ± SEM. n=60 cells from 3 biological replicates. Statistical comparisons were made using a one-way ANOVA with a Tukey's multiple comparison (ns not significant, **** P<0.0001). Scale bar, 20μm.

Fig. 2. Type I IFN treatment solely at time of infection inhibits LY294002-mediated reactivation of HSV-1 in primary sympathetic SCG neurons.

(**A**) Schematic of the primary postnatal sympathetic neuron-derived model of HSV-1 latency.

(**B**) Reactivation from latency is quantified by Us11-GFP expressing neurons following addition of the PI3K inhibitor LY294002 (20μM) in the presence of WAY-150168, which prevents cell-to-cell spread. The arrow indicates the time of LY294002 treatment at 5 days post-establishment of latency. n=9 biological replicates.

(**C**) Number of Us11-GFP expressing neurons at 3 days post-LY294002-induced reactivation in P6 SCG neuronal cultures infected with HSV-1 in the presence or absence of IFNα (600 IU/ml), then treated with an α-IFNAR1 neutralizing antibody. n=9 biological replicates.

(**D**) RT-qPCR for viral mRNA transcripts at 3 days post- LY294002-induced reactivation of SCGs infected with HSV-1 in the presence or absence of IFNα. n=9 biological replicates.
(**E**) RT-qPCR for viral mRNA transcripts at 20 hours post-LY294002-induced reactivation in SCGs infected with HSV-1 in the presence of absence of IFNα. n=9 biological replicates.
(**F**) Relative amount of viral DNA at time of reactivation (8dpi) in SCG neurons infected with HSV-1 in the presence or absence of IFNα (600 IU/ml). n=9 biological replicates.
(**G**) Quantification of vDNA foci detected by click chemistry at time of reactivation (8dpi) in SCG neurons infected with HSV-1 in the presence or absence of IFNα (600 IU/ml). n=60 genomes from 3 biological replicates.
(**H**) *LAT* mRNA expression at time of reactivation (8dpi) in neurons infected with HSV-1 in the presence or absence of IFNα (600 IU/ml). n=9 biological replicates.
Data information: Data represent the mean ± SEM. Statistical comparisons were made using a Mann-Whitney test (ns not significant, ** P<0.01, **** P<0.0001).

Fig. 3. Type I IFN-induced PML-NBs persist in primary sympathetic neurons despite resolution of IFN signaling.
(**A-C**) Kinetics of *ISG15*, *IRF7* and *PML* mRNA expression at 0.75, 1.75, 3.75 and 8.75 days post-IFNα (600 IU/ml) treatment. Arrow indicates the time of HSV-1 infection at 18hr post-interferon treatment. n=9 biological replicates.
(**D**) Quantification of PML puncta at 1-, 3-, 6-, 8-, 10- and 15-days post-infection with HSV-1 in untreated and IFNα (600 IU/ml)-treated SCG neurons. n≥60 cells from 3 biological replicates.
(**E**) Representative images of P6 SCG neurons treated with IFNα (600 IU/ml) and stained for STAT1 at 18 hours and 8 days post-treatment. Scale bar, 100μm.
(**F**) Representative images of P6 SCG neurons treated with IFNα (600 IU/ml) and stained for Mx1 at 18 hours and 6 days post-treatment. Scale bar, 20μm.

Data information: Data represent the mean ± SEM. Statistical comparisons were made using one-way ANOVA with a Tukey's multiple comparison (A-C) or mixed-effects analysis with a Tukey's multiple comparison (D). (ns not significant, ** P<0.01, **** P<0.0001).

Fig. 4. Type I IFN induced PML-NBs stably entrap vDNA throughout a latent HSV-1 infection of primary sympathetic neurons.

(**A**) Representative images of vDNA foci detected by click chemistry to PML at 1, 3, 6 and 8 dpi in P6 SCG neurons infected with HSV-1^{EdC} in the presence or absence of IFNα (600 IU/ml). Z-stack images of individual vDNA foci were acquired. Scale bar, 20μm. Zoom scale bar, 1 μm.

(**B**) Percent colocalization of vDNA foci detected by click chemistry to PML at 1, 3, 6 and 8 dpi in SCG neurons infected with HSV-1^{EdC} in the presence or absence of IFNα (600 IU/ml). Each point represents the percentage of 20 vDNA foci that colocalized to PML from 3 biological replicates.

(**C, D**) (C) 3D reconstruction of a high-resolution Z-series confocal image showing PML entrapment of a HSV-1^{EdC} vDNA foci. Scale bar, 2μm. (**D**) Enlargement of PML entrapped vDNA outlined by white dashed box. Scale bar, 0.5μm.

(**E**) Quantification of PML-NB volume in SCG neurons infected with HSV-1^{EdC} in the presence or absence of IFNα (600 IU/ml). n=64 biological replicates.

Data information: Data represent the mean ± SEM. Statistical comparisons were made using a 2way ANOVA (B) or a one way ANOVA with a Tukey's multiple comparison (E) (**** P<0.0001).

Fig. 5. HSV-1 genomes only associate with PML-NBs when type I IFN is present during initial infection.

(**A**) Number of Us11-GFP expressing P6 SCG neurons infected with HSV-1 following IFNα treatment for 18 hours prior to infection or for 18 hours at 3 days prior to infection. n=9 biological replicates.

(**B**) Percent colocalization of vDNA foci detected by click chemistry to PML at 8 dpi in SCG neurons infected with HSV-1^{EdC} following IFNα treatment for 18 hours prior to infection or for 18 hours at 3 days prior to infection. Each point represents the percentage of 20 vDNA foci that colocalized to PML from 3 biological replicates.

(**C**) Quantification of PML puncta at time of infection in P6 SCG neurons treated with IFNα (600 IU/ml) for 18 hours prior to infection or for 18hours at 3 days prior to infection. n=60 cells from 3 biological replicates.

(**D**) Percent colocalization of vDNA foci detected by click chemistry to PML at 3 dpi in SCG neurons with HSV-1^{EdC} infected with ICP0-null mutant HSV-1, n212, or a rescued HSV-1 virus, n212R, in P6 SCG neurons treated with IFNα for 18 hours prior to infection or for 18hours at 3 days prior to infection. Each point represents the percentage of 20 vDNA foci that colocalized to PML from 3 biological replicates.

Data information: Data represent the mean ± SEM. Statistical comparisons were made using a one way ANOVA with a Tukey's multiple comparison (A-C) or a 2way ANOVA (D) (ns not significant, ** P<0.01, **** P<0.0001).

Fig. 6. Depletion of PML with shRNA-mediated knockdown prior to infection restores HSV-1 reactivation in type I interferon-treated primary sympathetic neurons.

(**A**) Quantification of PML puncta in P6 SCG neurons transduced with either control non-targeting shRNA or shRNA targeting PML for 3 days, then treated with IFNα (600 IU/ml) for 18 hours. n=60 cells from 3 biological replicates.

(**B**) Quantification of colocalization of vDNA foci detected by click chemistry to PML in primary SCG neurons transduced with shRNA targeting PML for 3 days prior to being infected with

HSV-1^{EdC} in the presence or absence of IFNα (150 IU/ml). Each point represents the percentage of 20 vDNA foci that colocalized to PML from 3 biological replicates.

(**C-F**) Number of Us11-GFP expressing neurons at 3 days post-LY294002-induced reactivation in P6 SCG neuronal cultures transduced with shRNA targeting PML for 3 days prior to infection with HSV-1 in the presence or absence of IFNα (150 IU/ml). n=9 biological replicates.

Data information: Data represent the mean ± SEM. Statistical comparisons were made using a one way ANOVA with a Tukey's multiple comparison (ns not significant, ** P<0.01, **** P<.0001).

Fig. 7. Depletion of PML with shRNA mediated knockdown post-infection partially restores LY294002-mediated HSV-1 reactivation in type I interferon-treated primary sympathetic neurons.

(**A-D**) Number of Us11-GFP expressing neurons at 3 days post-LY294002-induced reactivation in P6 SCG neuronal cultures transduced with shRNA targeting PML at 1 day post-infection with HSV-1 in the presence or absence of IFNα (150 IU/ml). n=9 biological replicates. Statistical comparisons were made using a Mann-Whitney test (ns not significant, * P<0.05).

(**E**) Quantification of colocalization of vDNA foci detected by click chemistry to PML in primary SCG neurons transduced with shRNA targeting PML at 1 day post-infection with HSV-1^{EdC} in the presence or absence of IFNα (150 IU/ml). Each point represents the percentage of 20 vDNA foci that colocalized to PML from 3 biological replicates.

(**F**) Number of Us11-GFP expressing neurons at 3 days post- reactivation in P6 SCG neuronal cultures transduced with shRNA targeting PML at 1 day post-infection with HSV-1 in the presence of IFNα (150 IU/ml). Reactivation was induced by LY294002 in the presence of the DLK inhibitor GNE-3511 (4μM). n=9 biological replicates.

Data information: Data represent the mean ± SEM. Statistical comparisons were made using a Mann-Whitney test (A-E) or a one way ANOVA with a Tukey's multiple comparison (F) (ns not significant, * P<0.05, **** P<.0001).

Expanded View Figure Legends

Fig. EV1. Type I IFN alters the sub-cellular localization of ATRX, Daxx and SUMO-1 in primary peripheral neurons.

(**A**) Representative images of P6 SCG neurons treated with IFNβ (150 IU/ml) and stained for PML and ATRX.

(**B**) Representative images of P6 SCG treated with IFNα (600 IU/ml), IFNγ (500 IU/ml) and IFNλ2 (500 ng/ml) and stained for PML.

(**C**) Representative images of P6 TG treated with IFNα (600 IU/ml), IFNγ (500 IU/ml) and IFNλ2 (500 ng/ml) and stained for PML.

(D-F) Representative images of untreated or IFNα (600 IU/ml)-treated P6 SCG neurons stained for PML and ATRX (D), Daxx and ATRX (E) and PML and SUMO-1 (F). P6 dermal fibroblasts (DF) isolated from the same mice were used as a non-neuronal control (D-F).

Data information: Scale bars, 20μm.

Fig EV2. Type I IFN treatment solely at time of infection inhibits LY294002-mediated reactivation of HSV-1 in primary sympathetic SCG neurons.

(**A**) RT-qPCR for *ISG15* mRNA expression in SCG neurons treated with IFNα (600IU/ml) in the presence or absence of anti-mouse IFNAR-1 antibody (1:1000). n=6 biological replicates.

(**B, C**) RT-qPCR for viral mRNA transcripts at 3 days post-LY294002-induced reactivation of SCGs infected with HSV-1 in the presence or absence of IFNα (600 IU/ml). n=9 biological replicates.

(**D, E**) RT-qPCR for viral mRNA transcripts at 20 hours post- LY294002-induced reactivation in SCGs infected with HSV-1 in the presence or absence of IFNα (600 IU/ml). n=9 biological replicates.

Data information: Data represent the mean ± SEM. Statistical comparisons were made using a one way ANOVA with a Tukey's multiple comparison (A) or a Mann-Whitney test (ns not significant, *** P<0.001, **** P<0.0001).

Fig. EV3. PML-NBs entrap vDNA in the absence of type I IFN during lytic HSV-1 infection of murine dermal fibroblasts.

(**A**) Representative images of vDNA foci detected by click chemistry to PML at 60 minutes post-infection in P6 dermal fibroblasts lytically infected with HSV-1^{EdC} in the presence or absence of IFNα (600 IU/ml). Scale bar, 20μm. Zoom scale bar, 1μm.

(**B**) Percent colocalization of vDNA foci detected by click chemistry to PML at 60mpi in P6 dermal fibroblasts infected with HSV-1^{EdC} in the presence or absence of IFNα (600 IU/ml). Each point represents the percentage of 20 vDNA foci that colocalized to PML from 3 biological replicates.

Data information: Data represent the mean ± SEM. Statistical comparisons were made using a a Mann-Whitney test (ns not significant).

Fig EV4. HSV-1 genomes only associate with PML-NBs when type I IFN is present during initial infection.

(**A**) Representative images of untreated or IFNα-treated (600 IU/ml) P6 SCG neurons stained for PML and ATRX at 3 days post-treatment.

(**B**) Representative images of untreated or IFNα-treated (600 IU/ml) P6 SCG neurons stained for Daxx and ATRX at 3 days post-treatment.

(**C**) Representative images of untreated or IFNα-treated (600 IU/ml) P6 SCG neurons stained for PML and SUMO-1 at 3 days post-treatment.

(D) Percent colocalization of vDNA foci detected by click chemistry to PML at 3 dpi in SCG neurons infected with HSV-1^{EdC} with or without IFNα (600 IU/ml) present at the time of infection. Each point represents the percentage of 20 vDNA foci that colocalized to PML from 3 biological replicates.

(**E, F**) Representative images of HSV-1-infected P6 SCG neurons treated with IFNα (600 IU/ml) for 18 hours prior to infection or for 18hours at 3 days prior to infection and stained for ICP0 and ATRX at 3, 6 and 9 hours post-infection.

(**G**) Representative images of P6 SCG neurons infected with n212 or n212R for 8 hours and stained for HSV-1 ICP0.

Data information: Scale bars, 20μm. Data represent the mean ± SEM. Statistical comparisons were made using a a Mann-Whitney test (*** P<0.001).

Fig. EV5. PML is not required for ISG induction in primary postnatal sympathetic neurons.

(**A**) P6 SCG neurons were transduced with either control non-targeting shRNA or shRNA targeting PML for 3 days, then treated with IFNα (600 IU/ml) for 18 hours. Total genes >1.5-fold higher in IFNα (600 IU/ml) treated cells than untreated cells were subdivided into 3 groups: shCtrl-treated neurons only. shPML-treated neurons only. Both shCtrl and shPML neurons (shared).

(**B**) Gene expression heat map of top 50 most upregulated genes in P6 neurons transduced with control non-targeting shRNA or shRNA targeting PML for 3 days, then treated with IFNα (600 IU/ml) for 18 hours.

(**C**) Heat map of the top 25 shared upregulated GO terms in P6 neurons transduced with control non-targeting shRNA or shRNA targeting PML for 3 days, then treated with IFNα for 18 hours.

(**D, E**) RT-qPCR for *Pml* mRNA expression in SCG neurons transduced with either control non-targeting shRNA or shRNA targeting PML for 3 days, then treated with IFNα (600 IU/ml) for 18 hours. n=9 biological replicates.

(**F**) Quantification of detectable, IFNα (600 IU/ml)-induced PML puncta in P6 SCG neurons treated with ATO (1μM) for 2, 6, 18 and 24 hours. n=20 cells from 2 biological replicates.

(**G**) Number of Us11-GFP expressing neurons at 3 days post-treatment with LY294002 (20μM), ATO (1μM) or LY294002 (20μM) + ATO (1μM) in P6 SCG neuronal cultures infected with HSV-1 in the presence or absence of IFNα (600 IU/ml). n=12 biological replicates.

Data information: Data represent the mean ± SEM. Statistical comparisons were made using a one way ANOVA with a Tukey's multiple comparison (D-F) or a 2way ANOVA (G) (ns not significant, *** P<0.001, **** P<.0001).

Table 1: Compounds Used and Concentrations

Compound	Supplier	Identifier	Concentration
Acycloguanosine	Millipore Sigma	A4669	10 μM, 50 μM
FUDR	Millipore Sigma	F-0503	20 μM
L-Glutamic Acid	Millipore Sigma	G5638	3.7 μg/mL
LY 294002	Tocris	1130	20 μM
IFNα	EMD Millipore	IF009	150 IU/ml, 600 IU/ml
IFNβ	EMD Millipore	IF011	150 IU/ml
IFNγ	EMD Millipore	IF005	150 IU/ml, 500 IU/ml
IFNλ2	PeproTech	250-33	100 ng/ml, 500 ng/ml
NGF 2.5S	Alomone Labs	N-100	50 ng/mL
Primocin	Invivogen	ant-pm-1	100 μg/mL
Aphidicolin	AG Scientific	A-1026	3.3 μg/mL
WAY-150138	Pfizer	N/A	10 μg/mL
AFDye 555 Azide Plus	Click Chemistry Tools	1479-1	10μM

Table 2: Primers Used for RT-qPCR

Primer	Sequence 5’ to 3’
mGAP 1SF	CAT GGC CTT CCG TGT GTT CCT A
mGAP 1SR	GCG GCA CGT CAG ATC CA
ICP27 F	GCA TCC TTC GTG TTT GTC ATT CTG
ICP27 R	GCA TCT TCT CTC CGA CCC CG
ICP8 1SF	GGA GGT GCA CCG CAT ACC
ICP8 1SR	GGC TAA AAT CCG GCA TGA AC
gC #1 F	GAG TTT GTC TGG TTC GAG GAC
gC #1R	ACG GTA GAG ACT GTG GTG AA
PML F	GGG AAA CAG AGG AGC GAG TT
PML R	AAG GCC TTG AGG GAA TTG GG
ISG15 F	CAA GCA GCC AGA AGC AGA CT
ISG15 R	CCC AGC ATC TTC ACC TTT AGG
IRF7 F	CCA GTT GAT CCG CAT AAG GT
IRF7 R	GAG GCT CAC TTC TTC CCT ATT T
LAT F	TGT GTG GTG CCC GTG TCT T
LAT R	CCA GCC AAT CCG TGT CGG

Table 3: Antibodies Used for Immunofluorescence and Concentrations

Antibody	Supplier	Identifier/ RRID	Concentration
Anti-PML Mouse monoclonal	EMD Millipore	MAB3738 AB_2166836	1:200
Anti-Beta-III Tubulin Chicken polyclonal	Millipore sigma	AB9354 AB_570918	1:500
Anti-ATRX Rabbit polyclonal	Santa Cruz Bio	sc-15408 AB_2061023	1:250
Anti-Daxx Mouse monoclonal	Santa Cruz Bio	sc-8043 AB_627405	1:250
Anti-STAT1 Rabbit monoclonal	Cell Signaling Technologies	14994 AB_2737027	1:400
Anti-Mx1/2/3 Mouse monoclonal	Santa Cruz Bio	sc-166412 AB_2147714	1:250
Anti-HSV-1 ICP0 Mouse monoclonal	East Coast Bio	H1A027	1:200
Anti-SUMO-1 Rabbit monoclonal	Abcam	Ab32058 AB_778173	1:250
Anti-IFNAR-1 Mouse monoclonal	Leinco Tech	I-1188 AB_2830518	1:1000
F(ab')2 Anti-Mouse IgG Alexa Fluor® 555 Goat polyclonal	Thermo Fisher	A21425 AB_2535846	1:1000
F(ab')2 Anti-Rabbit IgG Alexa Fluor® 488 Goat polyclonal	Thermo Fisher	A11070 AB_2534114	1:1000
F(ab')2 Anti-Rabbit IgG Alexa Fluor® 488 Goat polyclonal	Thermo Fisher	A11017 AB_2534084	1:1000
Anti-Chicken IgY Alexa Fluor® 647 Goat polyclonal	Abcam	ab150175 AB_2732800	1:1000

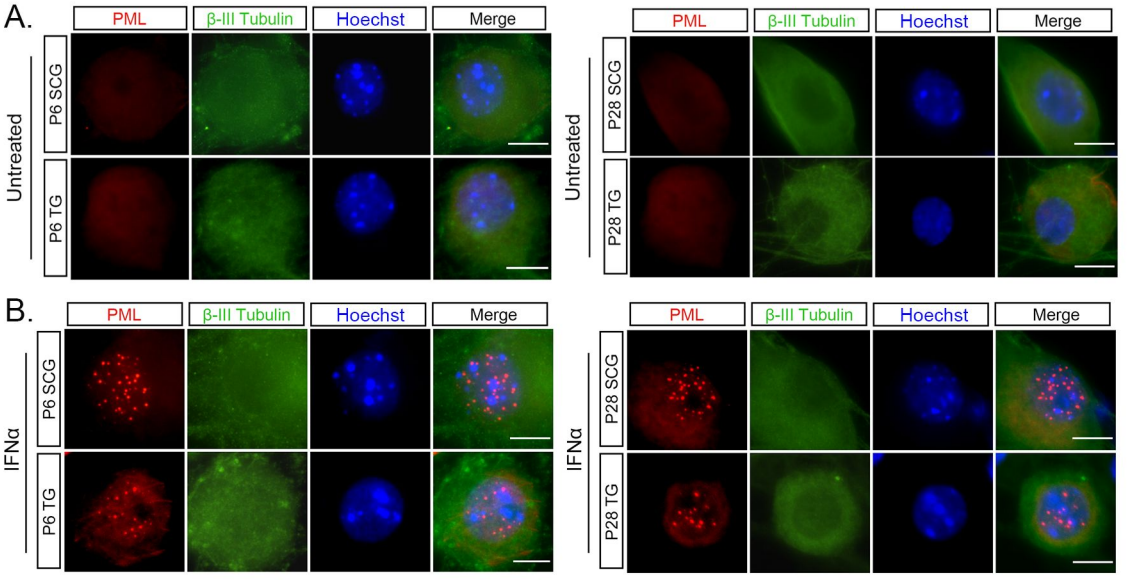
A.
PML
β-III Tubulin
Hoechst
Merge
Untreated
P6 SCG
P6 TG
P28 SCG
P28 TG
B.
IFNα

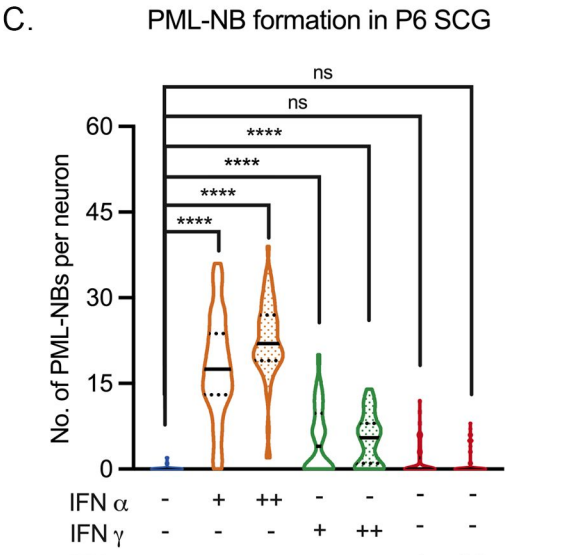
C.
PML-NB formation in P6 SCG
No. of PML-NBs per neuron
ns
****
IFN α
IFN γ
IFN λ2

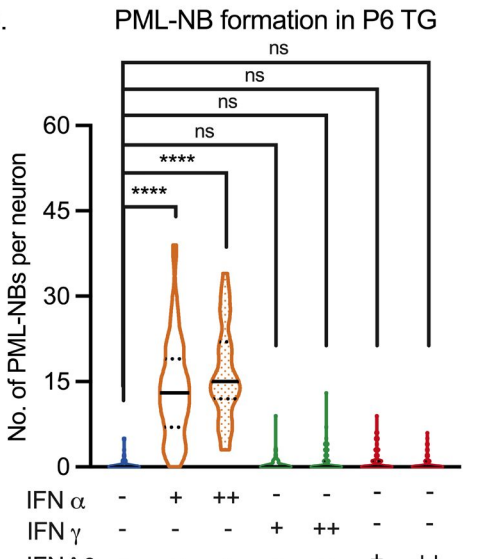
D.
PML-NB formation in P6 TG
No. of PML-NBs per neuron
ns
****
IFN α
IFN γ
IFN λ2

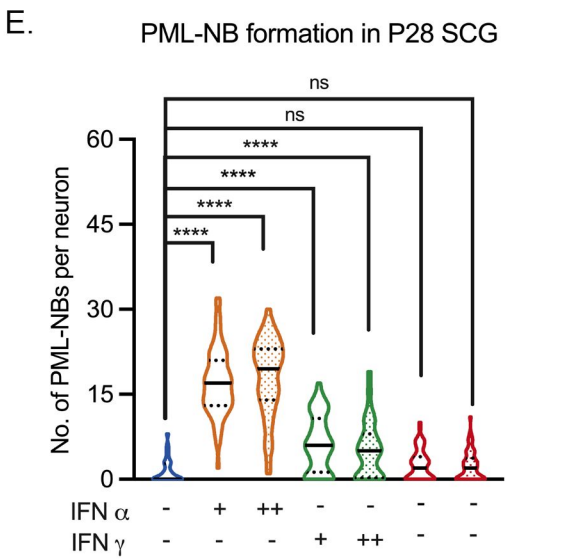
E.
PML-NB formation in P28 SCG
No. of PML-NBs per neuron
ns
****
IFN α
IFN γ
IFN λ2

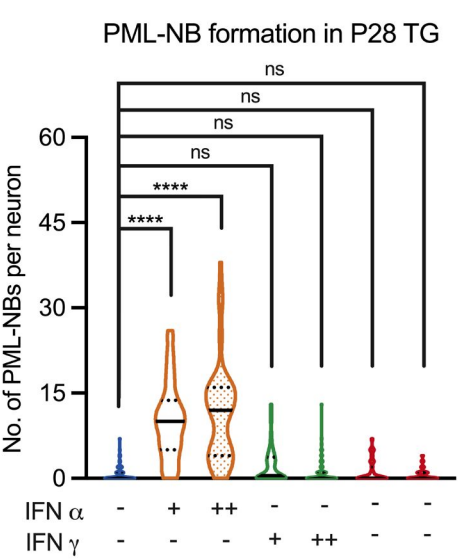
F.
PML-NB formation in P28 TG
No. of PML-NBs per neuron
ns
****
IFN α
IFN γ
IFN λ2

Figure 1

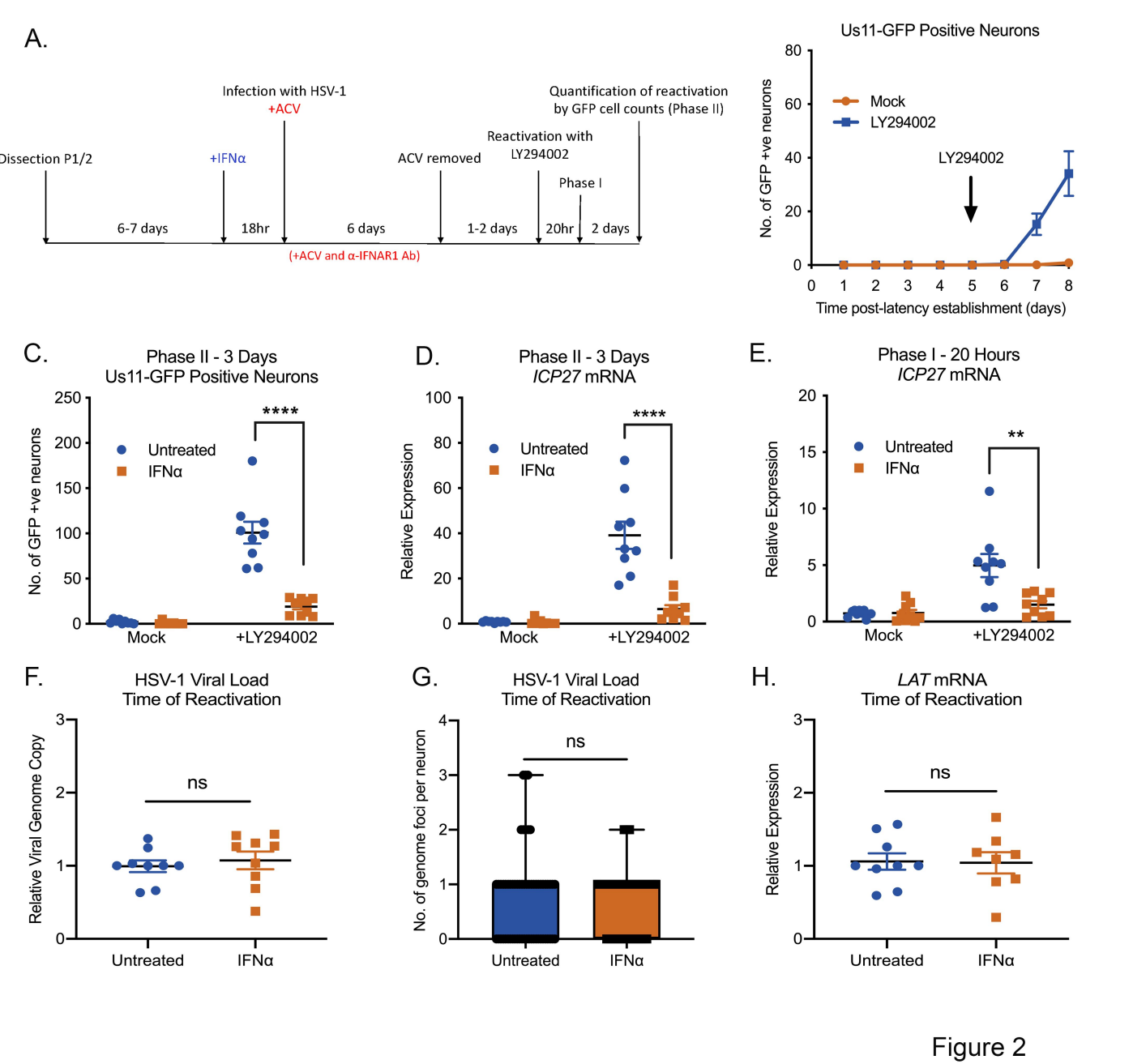
A.
Infection with HSV-1
+ACV
Quantification of reactivation
by GFP cell counts (Phase II)
Reactivation with
LY294002
Dissection P1/2
+IFNα
ACV removed
Phase I
6-7 days
18hr
6 days
1-2 days
20hr
2 days
(+ACV and α-IFNAR1 Ab)
Us11-GFP Positive Neurons
Mock
LY294002
LY294002
No. of GFP +ve neurons
Time post-latency establishment (days)
C.
Phase II - 3 Days
Us11-GFP Positive Neurons
Untreated
IFNα
****
No. of GFP +ve neurons
Mock
+LY294002
D.
Phase II - 3 Days
ICP27 mRNA
Untreated
IFNα
****
Relative Expression
Mock
+LY294002
E.
Phase I - 20 Hours
ICP27 mRNA
Untreated
IFNα
**
Relative Expression
Mock
+LY294002
F.
HSV-1 Viral Load
Time of Reactivation
ns
Relative Viral Genome Copy
Untreated
IFNα
G.
HSV-1 Viral Load
Time of Reactivation
ns
No. of genome foci per neuron
Untreated
IFNα
H.
LAT mRNA
Time of Reactivation
ns
Relative Expression
Untreated
IFNα

Figure 2

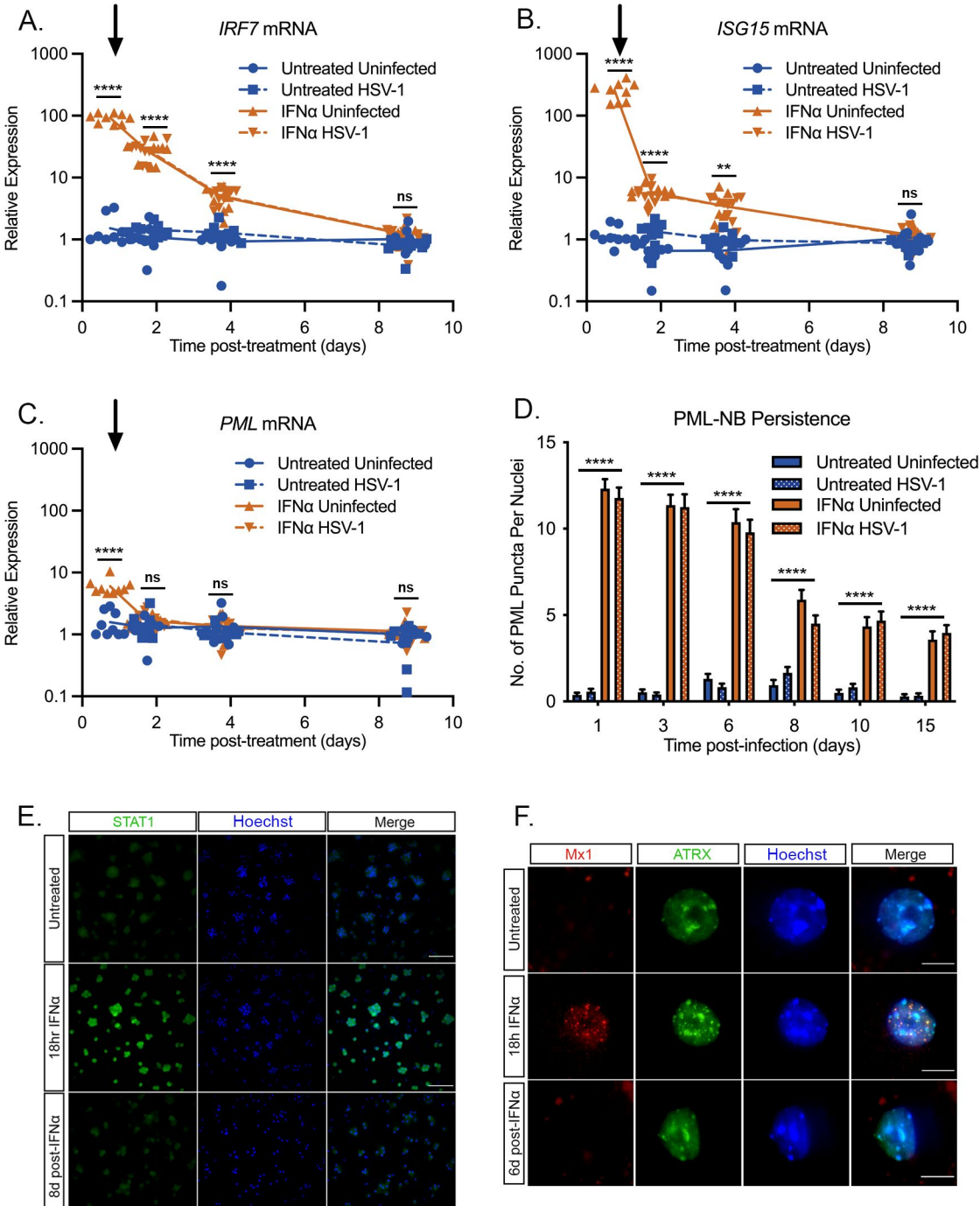
A.
IRF7 mRNA
Untreated Uninfected
Untreated HSV-1
IFNα Uninfected
IFNα HSV-1
Relative Expression
Time post-treatment (days)
B.
ISG15 mRNA
C.
PML mRNA
D.
PML-NB Persistence
No. of PML Puncta Per Nuclei
Time post-infection (days)
E.
STAT1
Hoechst
Merge
Untreated
18hr IFNα
8d post-IFNα
F.
Mx1
ATRX
18h IFNα
6d post-IFNα

Figure 3

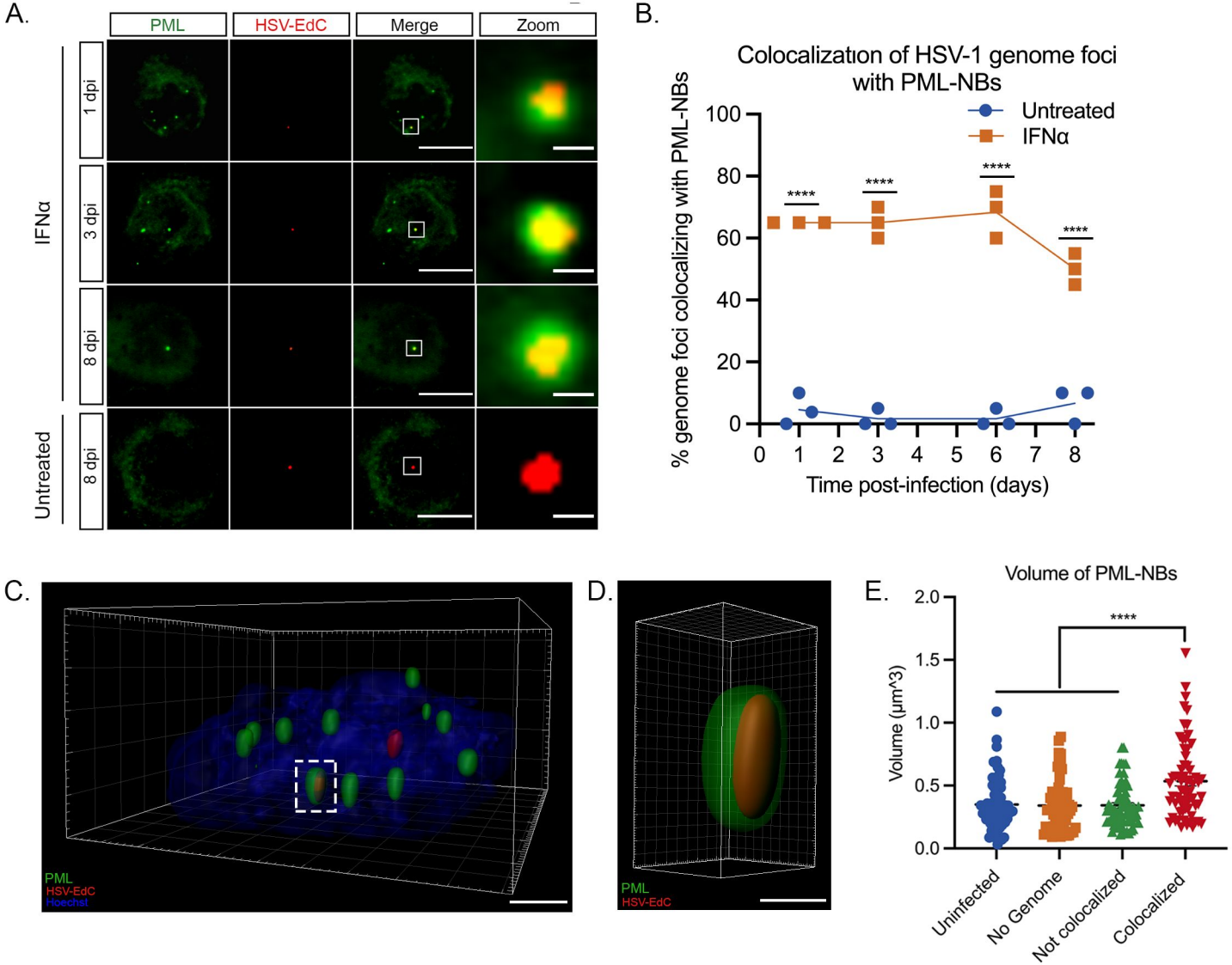
A.
PML
HSV-EdC
Merge
Zoom
IFNα
1 dpi
3 dpi
8 dpi
Untreated
8 dpi
B.
Colocalization of HSV-1 genome foci with PML-NBs
Untreated
IFNα
% genome foci colocalizing with PML-NBs
Time post-infection (days)
****
C.
PML
HSV-EdC
Hoechst
D.
PML
HSV-EdC
E.
Volume of PML-NBs
Volume (μm^3)
Uninfected
No Genome
Not colocalized
Colocalized

Figure 4

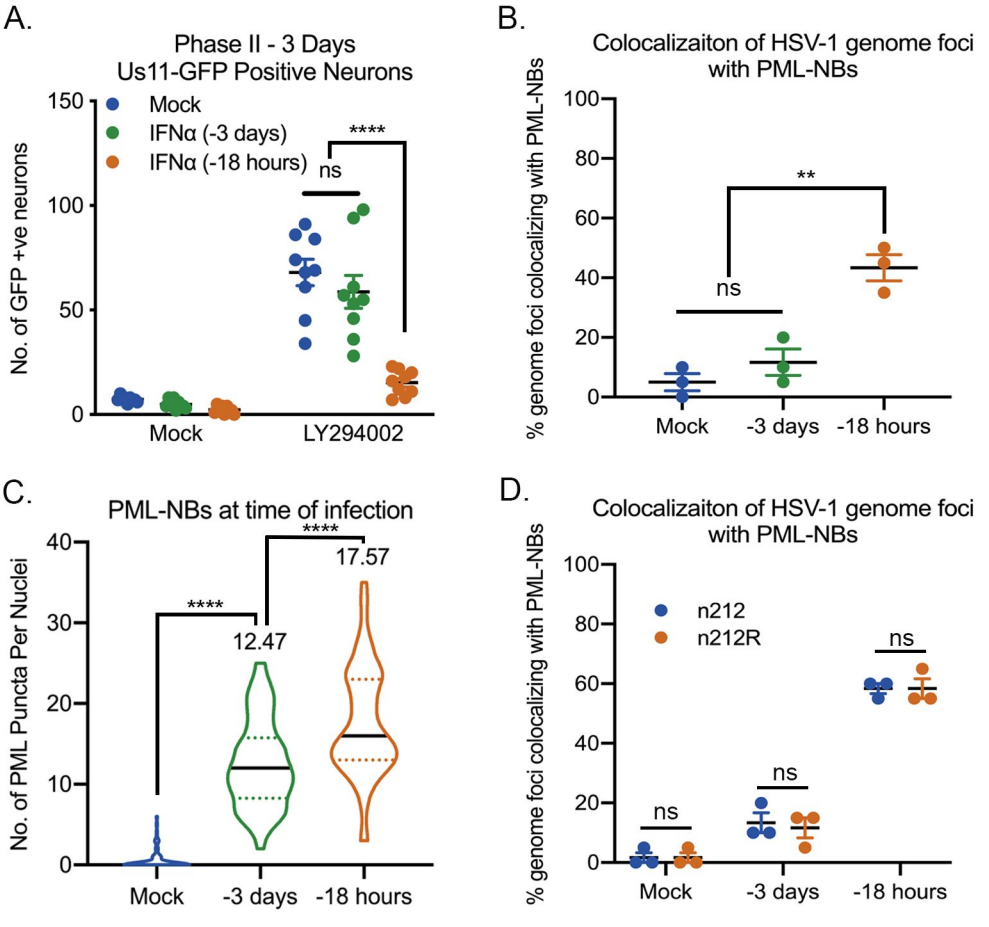
A.
Phase II - 3 Days
Us11-GFP Positive Neurons
Mock
IFNα (-3 days)
IFNα (-18 hours)
No. of GFP +ve neurons
150
100
50
0
****
ns
Mock
LY294002
B.
Colocalizaiton of HSV-1 genome foci
with PML-NBs
% genome foci colocalizing with PML-NBs
100
80
60
40
20
0
**
ns
Mock
-3 days
-18 hours
C.
PML-NBs at time of infection
No. of PML Puncta Per Nuclei
40
30
20
10
0
****
****
12.47
17.57
Mock
-3 days
-18 hours
D.
Colocalizaiton of HSV-1 genome foci
with PML-NBs
% genome foci colocalizing with PML-NBs
n212
n212R
100
80
60
40
20
0
ns
ns
ns
Mock
-3 days
-18 hours

Figure 5

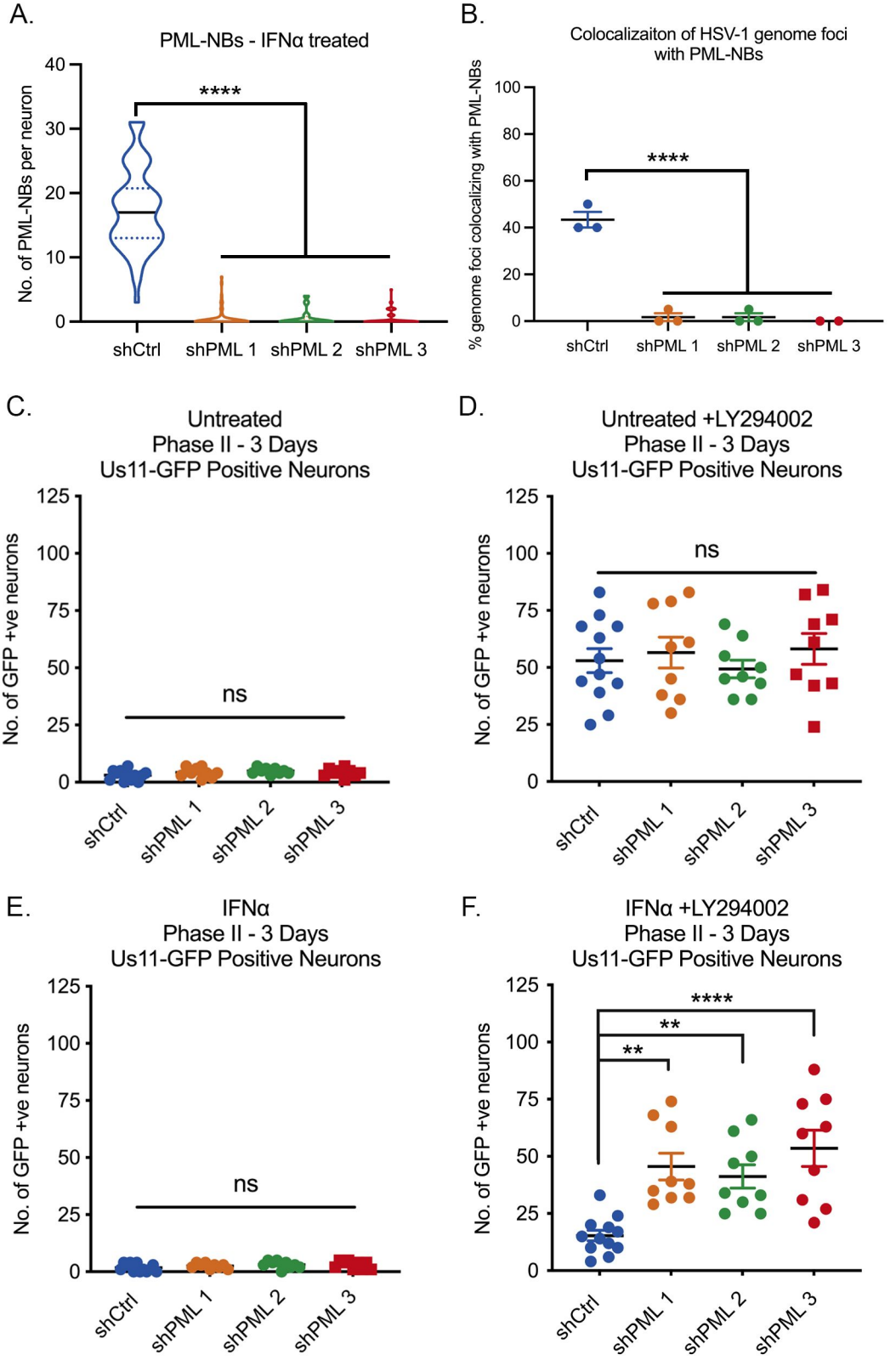
A.
PML-NBs - IFNα treated
No. of PML-NBs per neuron
40
30
20
10
0
****
shCtrl
shPML 1
shPML 2
shPML 3
B.
Colocalizaiton of HSV-1 genome foci with PML-NBs
% genome foci colocalizing with PML-NBs
100
80
60
40
20
0
****
shCtrl
shPML 1
shPML 2
shPML 3
C.
Untreated
Phase II - 3 Days
Us11-GFP Positive Neurons
No. of GFP +ve neurons
125
100
75
50
25
0
ns
shCtrl
shPML 1
shPML 2
shPML 3
D.
Untreated +LY294002
Phase II - 3 Days
Us11-GFP Positive Neurons
No. of GFP +ve neurons
125
100
75
50
25
0
ns
shCtrl
shPML 1
shPML 2
shPML 3
E.
IFNα
Phase II - 3 Days
Us11-GFP Positive Neurons
No. of GFP +ve neurons
125
100
75
50
25
0
ns
shCtrl
shPML 1
shPML 2
shPML 3
F.
IFNα +LY294002
Phase II - 3 Days
Us11-GFP Positive Neurons
No. of GFP +ve neurons
125
100
75
50
25
0
****
**
**
shCtrl
shPML 1
shPML 2
shPML 3

Figure 6

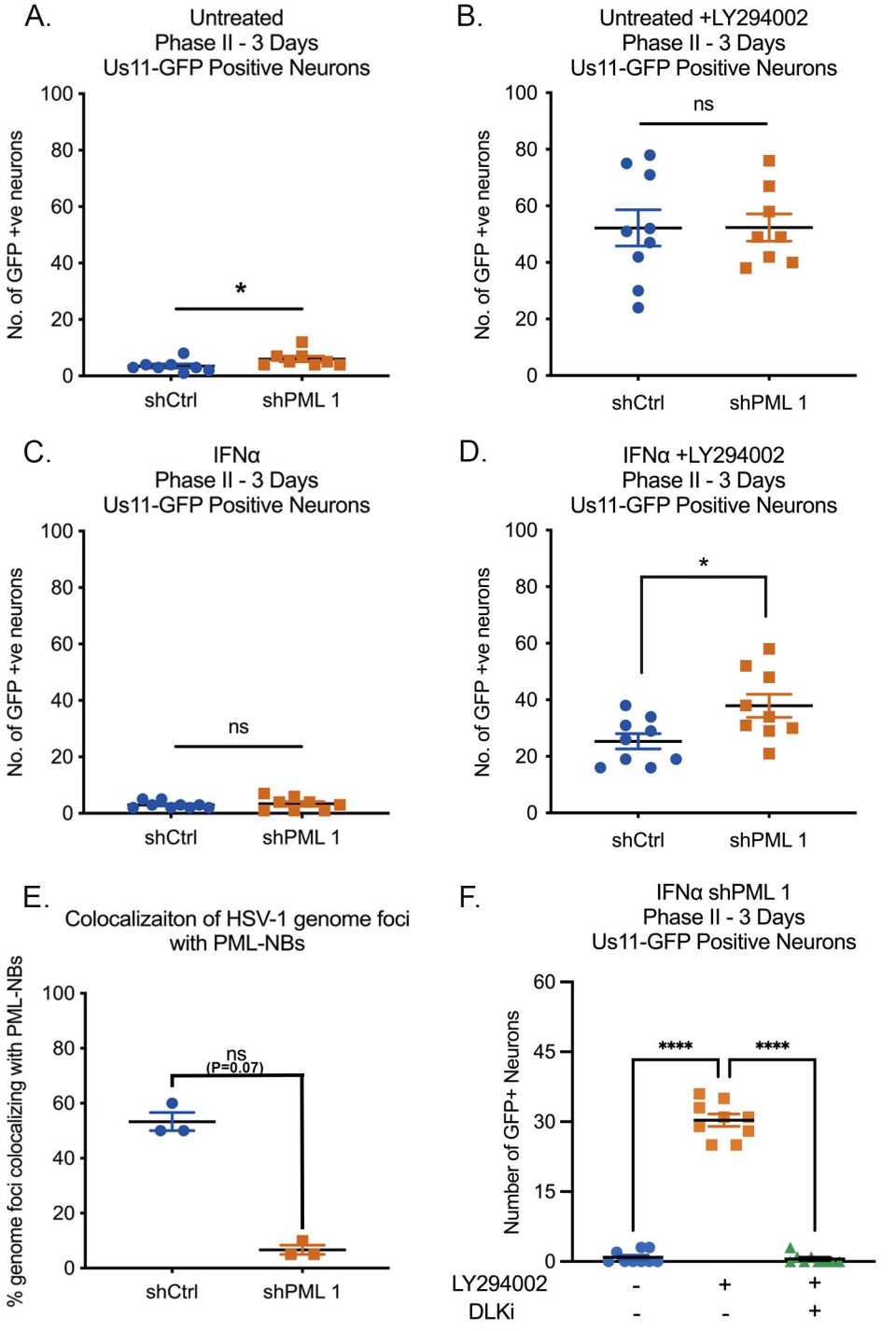
A.
Untreated
Phase II - 3 Days
Us11-GFP Positive Neurons
No. of GFP +ve neurons
100
80
60
40
20
0
*
shCtrl
shPML 1
B.
Untreated +LY294002
Phase II - 3 Days
Us11-GFP Positive Neurons
No. of GFP +ve neurons
ns
shCtrl
shPML 1
C.
IFNα
Phase II - 3 Days
Us11-GFP Positive Neurons
No. of GFP +ve neurons
ns
shCtrl
shPML 1
D.
IFNα +LY294002
Phase II - 3 Days
Us11-GFP Positive Neurons
No. of GFP +ve neurons
*
shCtrl
shPML 1
E.
Colocalizaiton of HSV-1 genome foci
with PML-NBs
% genome foci colocalizing with PML-NBs
ns
(P=0.07)
shCtrl
shPML 1
F.
IFNα shPML 1
Phase II - 3 Days
Us11-GFP Positive Neurons
Number of GFP+ Neurons
60
45
30
15
0
****
****
LY294002
DLKi
- + +
- - +

Figure 7

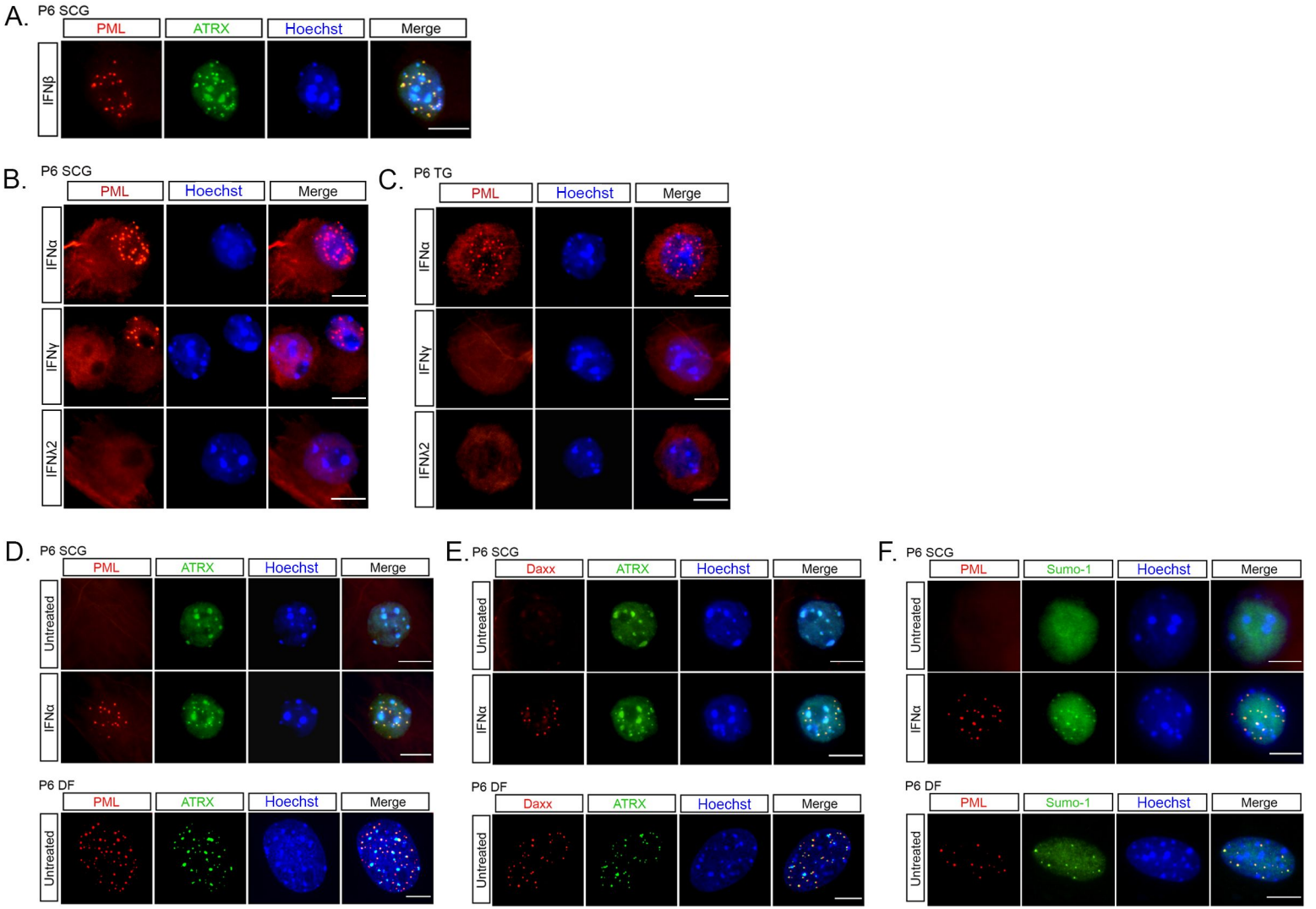
A.
P6 SCG
PML
ATRX
Hoechst
Merge
IFNβ
B.
P6 SCG
PML
Hoechst
Merge
IFNα
IFNγ
IFNλ2
C.
P6 TG
PML
Hoechst
Merge
IFNα
IFNγ
IFNλ2
D.
P6 SCG
PML
ATRX
Hoechst
Merge
Untreated
IFNα
P6 DF
PML
ATRX
Hoechst
Merge
Untreated
E.
P6 SCG
Daxx
ATRX
Hoechst
Merge
Untreated
IFNα
P6 DF
Daxx
ATRX
Hoechst
Merge
Untreated
F.
P6 SCG
PML
Sumo-1
Hoechst
Merge
Untreated
IFNα
P6 DF
PML
Sumo-1
Hoechst
Merge
Untreated

Figure EV1

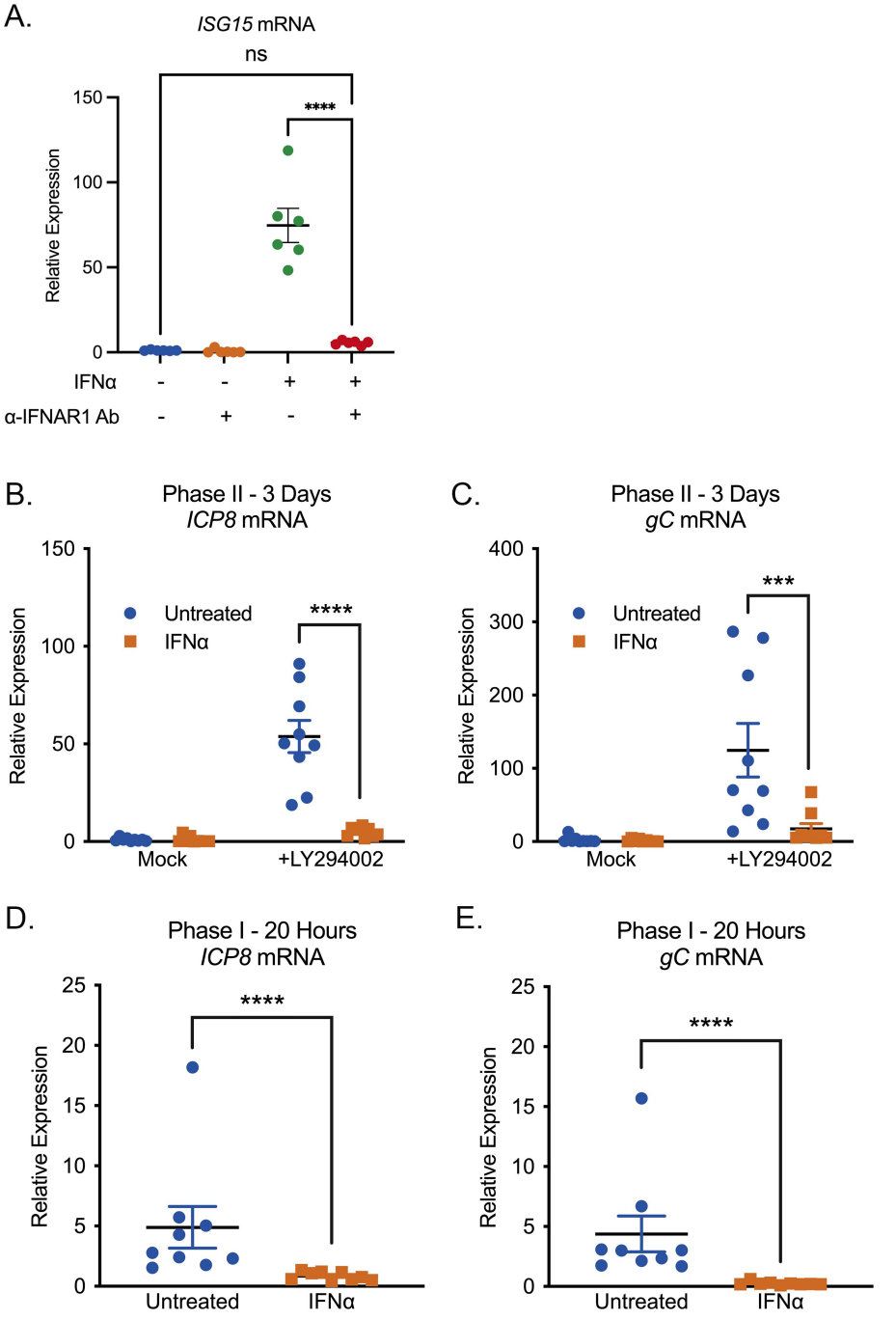
A.
ISG15 mRNA
ns
****
Relative Expression
150
100
50
0
IFNα - - + +
α-IFNAR1 Ab - + - +
B.
Phase II - 3 Days
ICP8 mRNA
Untreated
IFNα
****
Relative Expression
150
100
50
0
Mock
+LY294002
C.
Phase II - 3 Days
gC mRNA
Untreated
IFNα
***
Relative Expression
400
300
200
100
0
Mock
+LY294002
D.
Phase I - 20 Hours
ICP8 mRNA
****
Relative Expression
25
20
15
10
5
0
Untreated
IFNα
E.
Phase I - 20 Hours
gC mRNA
****
Relative Expression
25
20
15
10
5
0
Untreated
IFNα

Figure EV2

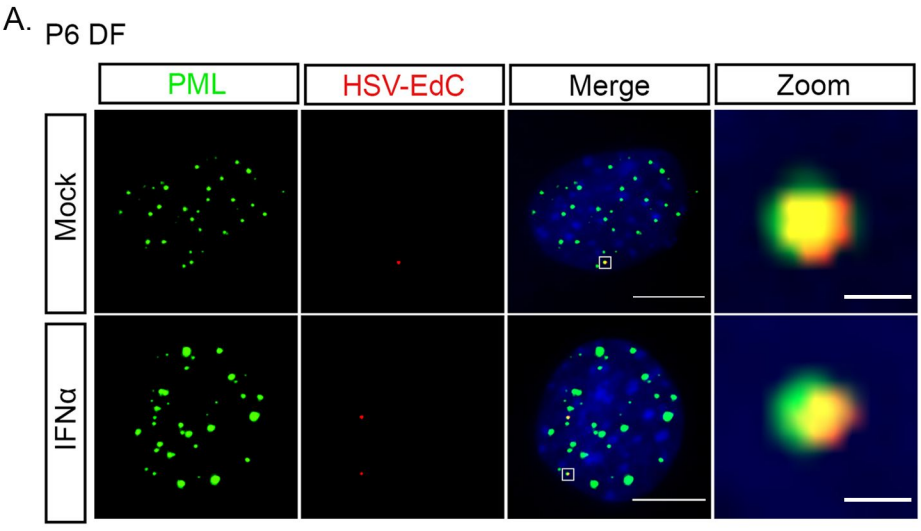
A.
P6 DF
PML
HSV-EdC
Merge
Zoom
Mock
IFNα

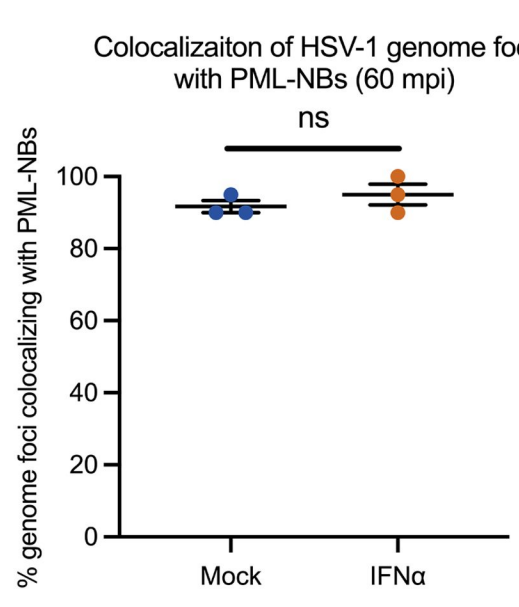
B.
Colocalizaiton of HSV-1 genome foci with PML-NBs (60 mpi)
ns
% genome foci colocalizing with PML-NBs
100
80
60
40
20
0
Mock
IFNα

Figure EV3

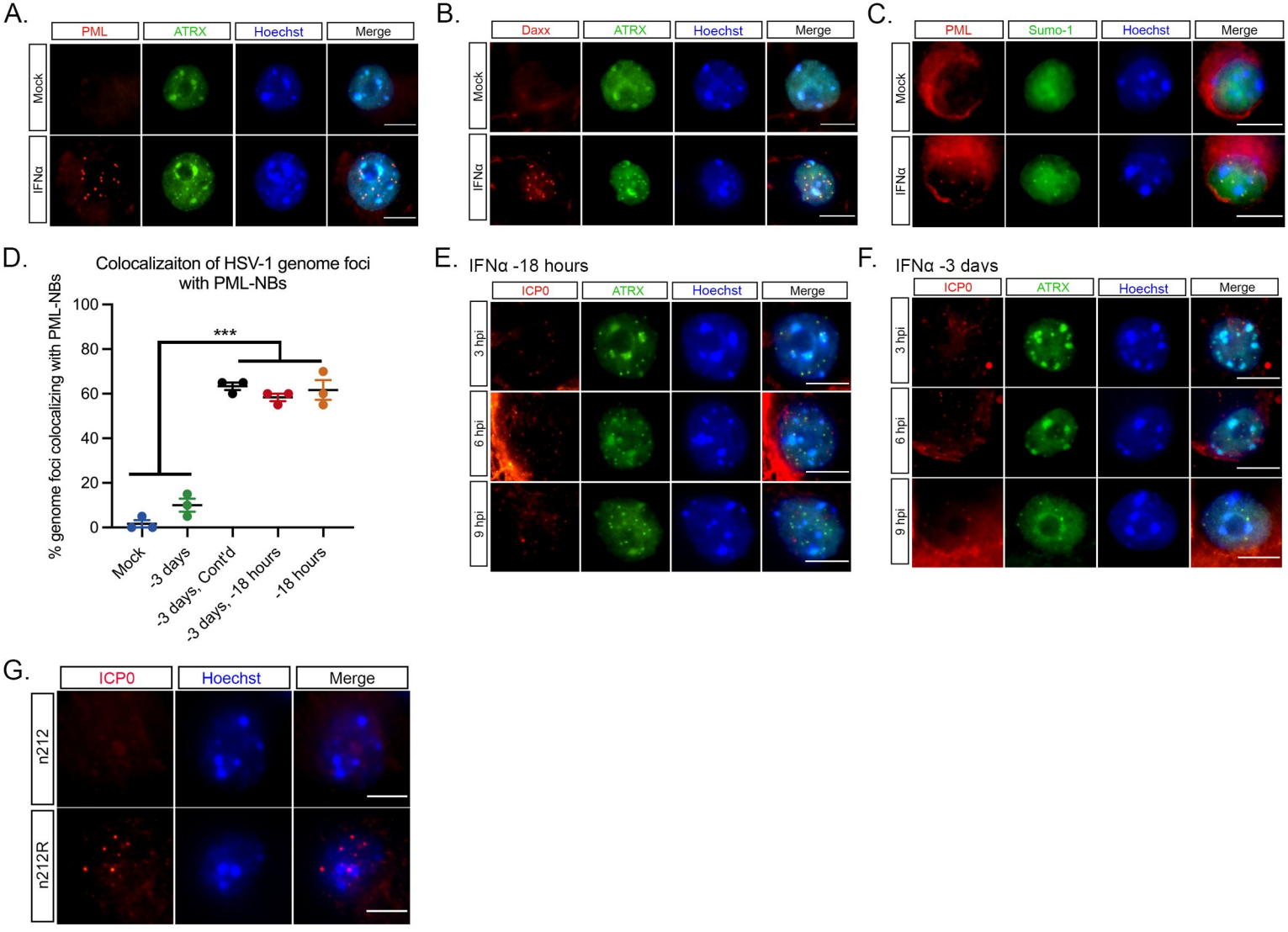
A.
PML
ATRX
Hoechst
Merge
Mock
IFNα
B.
Daxx
ATRX
Hoechst
Merge
Mock
IFNα
C.
PML
Sumo-1
Hoechst
Merge
Mock
IFNα
D.
Colocalizaiton of HSV-1 genome foci with PML-NBs
% genome foci colocalizing with PML-NBs
100
80
60
40
20
0
***
Mock
-3 days
-3 days; Cont'd
-3 days, -18 hours
-18 hours
E.
IFNα -18 hours
ICP0
ATRX
Hoechst
Merge
3 hpi
6 hpi
9 hpi
F.
IFNα -3 days
ICP0
ATRX
Hoechst
Merge
3 hpi
6 hpi
9 hpi
G.
ICP0
Hoechst
Merge
n212
n212R

Figure EV4

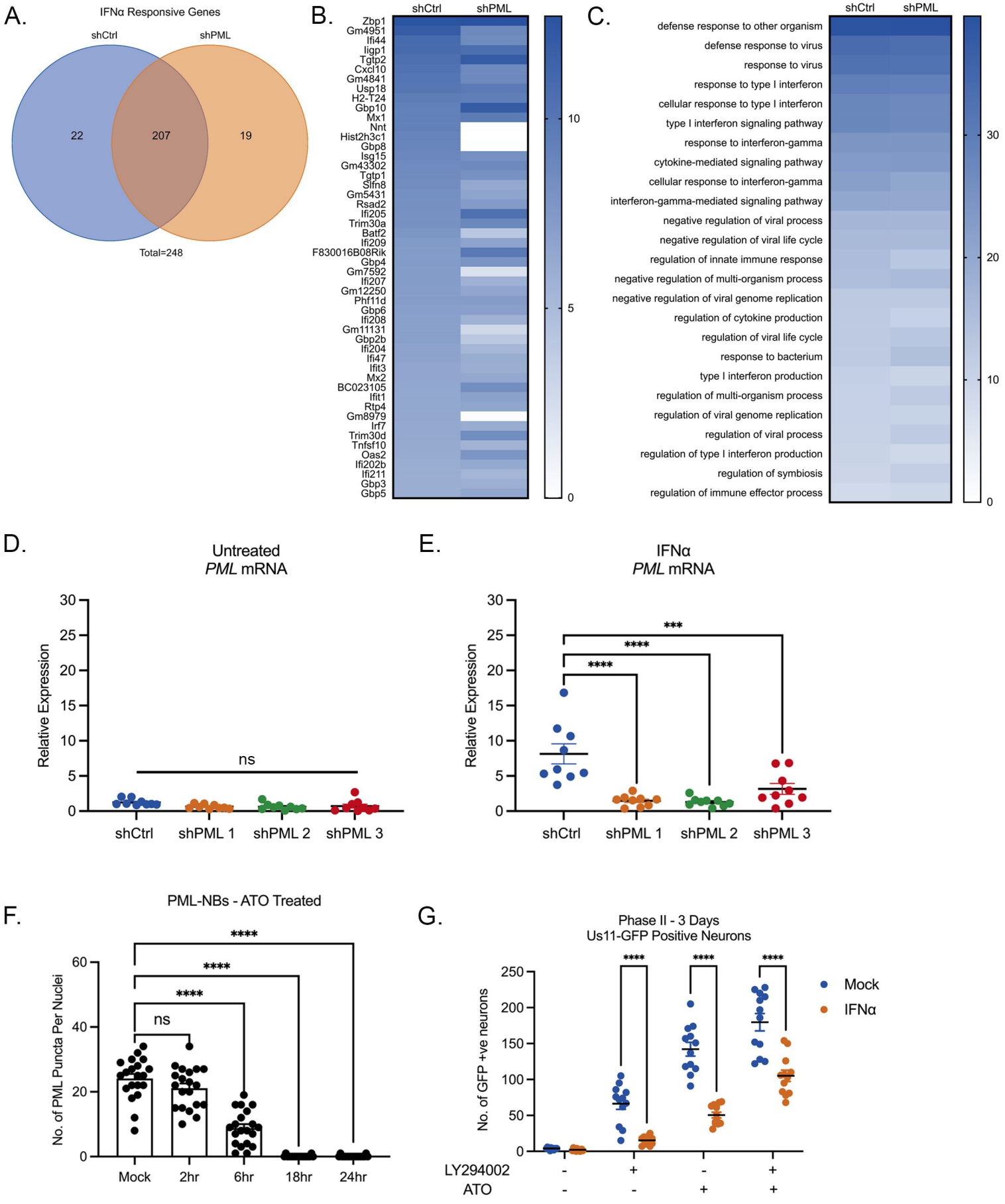
A.
IFNα Responsive Genes
shCtrl
shPML
22
207
19
Total=248
B.
shCtrl
shPML
Zbp1
Gm4951
Ifi44
Iigp1
Tgtp2
Cxcl10
Gm4841
Usp18
H2-T24
Gbp10
Mx1
Nnt
Hist2h3c1
Gbp8
Isg15
Gm43302
Tgtp1
Slfn8
Gm5431
Rsad2
Ifi205
Trim30a
Batf2
Ifi209
F830016B08Rik
Gbp4
Gm7592
Ifi207
Gm12250
Phf11d
Gbp6
Ifi208
Gm11131
Gbp2b
Ifi204
Ifi47
Ifit3
Mx2
BC023105
Ifit1
Rtp4
Gm8979
Irf7
Trim30d
Tnfsf10
Oas2
Ifi202b
Ifi211
Gbp3
Gbp5
10
5
0
C.
shCtrl
shPML
defense response to other organism
defense response to virus
response to virus
response to type I interferon
cellular response to type I interferon
type I interferon signaling pathway
response to interferon-gamma
cytokine-mediated signaling pathway
cellular response to interferon-gamma
interferon-gamma-mediated signaling pathway
negative regulation of viral process
negative regulation of viral life cycle
regulation of innate immune response
negative regulation of multi-organism process
negative regulation of viral genome replication
regulation of cytokine production
regulation of viral life cycle
response to bacterium
type I interferon production
regulation of multi-organism process
regulation of viral genome replication
regulation of viral process
regulation of type I interferon production
regulation of symbiosis
regulation of immune effector process
30
20
10
0
D.
Untreated
PML mRNA
Relative Expression
30
25
20
15
10
5
0
ns
shCtrl
shPML 1
shPML 2
shPML 3
E.
IFNα
PML mRNA
Relative Expression
30
25
20
15
10
5
0
***
****
****
shCtrl
shPML 1
shPML 2
shPML 3
F.
PML-NBs - ATO Treated
No. of PML Puncta Per Nuclei
60
40
20
0
****
****
****
ns
Mock
2hr
6hr
18hr
24hr
G.
Phase II - 3 Days
Us11-GFP Positive Neurons
No. of GFP +ve neurons
250
200
150
100
50
0
****
****
****
Mock
IFNα
LY294002
ATO
-
+
-
+
-
-
+
+

Figure EV5